ISSN 1063-7796, Physics of Particles and Nuclei, 2009, Vol. 40, No. 4, pp. 558–581. © Pleiades Publishing, Ltd., 2009.
Original Russian Text © Yu.B. Gurov, S.V. Lapushkin, B.A. Chernyshev, V.G. Sandukovsky, 2009, published in Fizika Elementarnykh Chastits i Atomnogo Yadra, 2009, Vol. 40, No. 4.

Search for Superheavy Hydrogen Isotopes in Pion Absorption Reactions

Yu. B. Gurov[a], S. V. Lapushkin[a], B. A. Chernyshev[a], and V. G. Sandukovsky[b]

[a] *Moscow Engineering Physics Institute (State University)*
[b] *Joint Institute for Nuclear Research, Dubna*

Abstract—Review of the experimental results on the search for and the spectroscopy of the superheavy hydrogen isotopes $^{4-7}$H obtained in stopped π^--meson absorption by ^{9}Be and ^{11}Be nuclei is presented. Study of light neutron-rich nuclei is a principal line in developing modern views on the properties of nuclear forces and determination of nuclear properties near the drip line. The present method of investigation relies on precision measurements of energy of charged particles emitted after pion absorption by nuclei. Important advantages of this method are the practically accurate initial state energy and momentum, as well as the possibility to study a wide range of excitation energy. In the frames of this method new results were obtained on level structures of the isotopes $^{4-6}$H and indications on ^{7}H production. Comparison with other experimental and theoretical results is performed.

PACS numbers: 25.80.Ls, 27.10.+h, 27.20.+n

DOI: 10.1134/S1063779609040054

INTRODUCTION

Experimental investigation of a level structure of light neutron-rich nuclei [1–4] is one of the main lines in developing modern ideas concerning the properties of nuclear forces, nuclear characteristics near the drip line, and the nature and origin of exotic nuclear states. A relatively small number of nucleons makes it possible to find a correct microscopic description of their properties and, therefore, to verify existing nuclear models as well as nucleon–nucleon potentials [5–9].

Superheavy hydrogen isotopes, among which the nuclei heavier than tritium are found, are the most interesting ones due to extremely large neutron–to–proton ratio and a proton 1*s*-shell being open, unlike that of other elements. Additional interest to superheavy hydrogen isotopes is caused by the fact that they are close enough to purely neutron nuclei whose existence has yet to be proven [10].

The experimental search for superheavy hydrogen isotopes and investigation of their level structure has been kept on going for a long time. Nevertheless, one has to admit that the experimental information available is still contradictory and, besides, for all nuclei, except for ^{4}H, is extremely limited.

In the present work a review of recent experimental results [11–16] on the search for and spectroscopy of the isotopes $^{4-7}$H obtained in stopped π^--meson absorption by ^{9}Be and ^{11}Be nuclei is given. The experiment was carried out in a high intensity low energy pion beam (LEP) of Los Alamos meson physics facility (LAMPF) using a two–arm semiconductor spectrometer of charged particles [17].

The outline of the review is as follows. In Chapter 1 the peculiarities of stopped π^--meson absorption reactions are considered which provide the possibility to investigate neutron–rich nuclei. In Chapter 2 a brief description of the experiment, conducted at LAMPF, is given. The results of the latter on the level structure of the isotopes $^{4-7}$H are presented in Chapter 3, as well as a comparison with experimental and theoretical results obtained by other authors. Special attention is paid to the results obtained recently with radioactive ion beams. In the conclusion open problems and further prospects of investigations are analyzed.

1. PRODUCTION OF NEUTRON-RICH ISOTOPES IN STOPPED π^--MESON ABSORPTION REACTIONS

An opportunity to effectively exploit stopped π^--meson absorption by nuclei to form neutron-rich nuclear states is based on the peculiarities of this reaction: a charge depletion of the nuclear system produced and a large energy release on a scale of nuclear excitations.

The principal features of stopped π^--meson absorption by atomic nuclei are firmly established [18]. The process of absorption itself proceeds through several stages. A low-energy pion, upon hitting a target, loses its kinetic energy as a result of ionization processes. After a while, a negatively charged pion is captured by the Coulomb field of the nucleus of one of the target atoms. At the same time, its initial orbital has a relatively large principal quantum number $n > 20$ [19]. Then, a pion experiences a number of consecutive transitions to orbitals with smaller values of n accompanied by the radiation of gamma quanta and Auger electrons.

An electromagnetic shower ceases when a pion gets absorbed from an orbital of the mesoatom as a result of the strong interactions. In the case of light elements, the pions are mainly absorbed from 1*s* and 2*p* levels. Notice that due to a relatively large lifetime ($\tau = 2.6 \times 10^{-8}$ s) nearly each pion stopped in a target gets absorbed by nucleus.

A distinctive feature of the method that uses reactions of stopped pion absorption is the absence of uncertainties due to the energy resolution and beam's angular divergence. The initial momentum of the system is strictly equal to zero. An uncertainty in the energy of the initial state results merely from a difference in binding energies between the ground, most bound, 1*s* state and 2*p* state, from which more than a half of pions are absorbed by considered nuclei. For ^{9}Be and ^{11}Be this difference is 0.042 and 0.066 MeV, respectively [19].

Absorption of a pion by nuclei is a multinucleon process [18]. A large energy release ($\sim m_\pi c^2$) leads to the production of several prompt nuclear particles, mainly neutrons, protons, deuterons, tritons, and helium isotopes ^{3,4}He, as well as a residual nucleus. The dominant mechanism is absorption by intranuclear a proton–nucleon pair with the deuteron quantum numbers ($J^p = 1^+$, $I = 0$, $I_{np} = 0$). A theoretical description of this process, as well as the process of absorption by the nucleon pair with other quantum numbers, is fairly well developed [18]. At the same time, a question concerning absorption mechanisms, which lead to two–particle channels and reactions with production of two energetic charged particles, is still a matter of debate. However, as will be shown below, lack of the corresponding theoretical models imposes almost no restrictions on the search for new nuclear states in two– and three–particle channels of reactions of pion absorption.

For those channels in which one or two charged particles are detected, a residual nucleus will be a neutron-rich one. In Tables 1 and 2 the nuclear states are presented which can be investigated in two– and three–particle channels of the reactions of π^--meson absorption by nuclei ^{9}Be and ^{11}Be.

It should be noted that the channel yields of the reactions, given in Tables 1 and 2, depend not only on the structure of isotopes, but also, to a great extent, on the mechanism of π^--meson capture reactions.

Two- and three-particle channels of neutron-rich nuclei production reveal themselves via peaks in the missing mass spectra for registering one and two particles, respectively. Note that as it follows from the phenomenological analysis of the experimental data [18], a sizeable contribution to pion absorption by nuclei is brought about by quasi–free processes in which the nucleons of residual nucleus do not immediately take part in the reaction. This favors a formation of loosely bound and quasi-stationary states in three-particle channels of the reaction, while the yield of the two-particle channel of the reaction almost on all nuclei is strongly suppressed.

Table 1. Residual nuclei produced in π^--meson absorption by nuclei ^{9}Be

Detected particles	*p*	*d*	*t*	^{3}He	^{4}He
Inclusive measurements	^{8}He	^{7}He	^{6}He	^{6}H	^{5}H
p	^{7}H	^{6}H	^{5}H	^{5}n	^{4}n
d	^{6}H	^{5}H	^{4}H	^{4}n	^{3}n
t	^{5}H	^{4}H	^{3}H	^{3}n	^{2}n
^{3}He	^{5}n	^{4}n	^{3}n	–	–
^{4}He	^{4}n	^{3}n	^{2}n	–	–

Table 2. Residual nuclei produced in π^--meson absorption by nuclei ^{11}B

Detected particles	*p*	*d*	*t*	^{3}He	^{4}He
Inclusive measurements	^{10}Li	^{9}Li	^{8}Li	^{8}He	^{7}He
p	^{9}He	^{8}He	^{7}He	^{7}H	^{6}H
d	^{8}He	^{7}He	^{6}He	^{6}H	^{5}H
t	^{7}He	^{6}He	^{5}He	^{5}H	^{4}H
^{3}He	^{7}H	^{6}H	^{5}H	^{5}n	^{4}n
^{4}He	^{6}H	^{5}H	^{4}H	^{4}n	^{3}n

Tables 1 and 2 demonstrate the important advantage of using the stopped reaction of pion absorption in the investigations of neutron-rich nuclei. A single experiment is sufficient to obtain information on the wide range of neutron-rich nuclei which comprise isotopes of helium and lithium, studied in detail, as well as poorly examined superheavy hydrogen isotopes and multineutrons, whose existence is still an open question. The data on the known nuclear states permit us to resolve in a natural way such problems as the energy calibration, the determination of the energy resolution, and the stability of the parameters of the experimental setup during data collecting.

It was shown in [20] that the nuclear fission process, induced by π^--meson absorption, can be used to synthesize new isotopes of both light and heavy elements. However, for a sufficiently long time experimental information was limited to superheavy hydrogen isotopes ^{4}H [21–29] and ^{5}H [27–29]. To a considerable degree, this is due to a long period of data collecting (~100 h) needed for acquiring sufficient statistics in high intensity pion beams of meson factories.

The experiment, carried out at LAMPF, yielded, in addition to information on superheavy hydrogen isotopes, new data on isotopes of helium ^{6}He [30], ^{7,8}He

[31], lithium ^{10}Li [31], ^{11}Li [32], ^{12}Li [33] and beryllium ^{13}Be [31].

Besides the advantages mentioned above the method proposed has its deficiencies. First of all, it is appropriate to note the lack of reliable theoretical models that describe the reactions studied. As a consequence, estimates of the background, which results from multiparticle channels of the reaction, have to be performed using phase space distributions. In the case of narrow states this approximation does not deteriorate the quality of results on the determination of the parameters of states obtained. However, as we will see later, the excitation spectrum of superheavy hydrogen isotopes is a set of wide overlapping resonances, and this demands additional investigation into the reliability of the results obtained.

Also, it is hard to look for breakup products of the state studied in the stopped reaction of pion absorption. This is due to their energies being extremely low. Hence, in the method considered it is quite difficult to determine quantum numbers of the state under investigation.

2. EXPERIMENT

The method of investigation of level structure of light nuclei near the drip line, that uses stopped π^--meson absorption reaction, was developed in a series of experiments done at PNPI synchrophasotron (Gatchina) in the late 1980's of the last century [34, 26, 27, 29, 35]. This method is based on the precision measurement of the energy of charged particles and was accomplished with the multilayer semiconductor telescopes possessing high energy resolution [36, 37]. Such devices make it possible to carry out inclusive as well as correlative measurements and achieve a reliable identification of the reaction products throughout the entire interval of energies of detected charged particles. Performing investigations in high intensity beams at meson factories and using thin targets in those experiments allows reaching unprecedentedly high statistics under conditions of high instrumental resolution.

First priority results concerning the spectroscopy of superheavy hydrogen isotopes ^{4}H and ^{5}H [26, 27, 29] were obtained in experiments carried out at PNPI on isotope–pure targets ^{9}Be and ^{6,7}Li. It should be noted that the existence of isotope ^{5}H was first observed in exactly these experiments in the reaction ^{9}Be(π^-, pt)X [38].

The results obtained at PNPI accelerator served a basis of the neutron-rich nuclei research program with stopped π^--meson absorption reactions, which was fulfilled at Los Alamos meson physics facility (LAMPF) (the experiment E1274 "Spectroscopy of Light Exotic Nuclei by a Novel Technique"). An improved energy resolution of the spectrometer (~three times higher) and statistics accumulated (~60 times higher), with respect to earlier measurements performed at PNPI, allowed obtaining fundamentally new results on the search for and spectroscopy of superheavy hydrogen isotopes.

In this chapter a brief description of a multilayer semiconductor spectrometer, along with the method of measurement of spectrum of charged particles produced in reactions of pion absorption, is given.

2.1. Experiment layout. The experiment was performed in the low energy pion (LEP) beam by the two-arm semiconductor spectrometer [17]. The layout of the experimental installation is sketched in Fig. 1. The beam of negatively charged pions with energy of 30 MeV passed through the beryllium degrader and stopped in the thin target. During deceleration approximately ~50% of the beam was stopped in beryllium, 5% in the target, nearly ~15% decayed in the vacuum chamber, and the remaining pions were absorbed by chamber walls. The rate at which pions were stopped in the target was $\sim 6 \times 10^4$ s^{-1}. The collimators C1 and C2 were used to suppress the background from secondary particles emitted by the degrader and chamber walls.

Those secondary charged particles were detected by two multilayer semiconductor devices (s.c.d. telescopes).

The following main goals were formulated in the process of spectrometer construction:

Achieve a high density of stopped particles in the target with reliable background suppression;

Provide sufficient aperture of the experiment installation;

Provide high energy resolution of detecting charged particles in the energy range from several to hundreds of MeV.

Five targets were used in the experiment: ^{9}Be, ^{10,11}B, and ^{12,14}C, which were made in the form of discs with diameter 26 mm and thickness ~ 25 mg/cm^2. The targets, which were fixed by thin fibers (30 μm) made of beryllium bronze, were located at a distance of 4.5 cm from the degrader and at 22° with respect to the beam axis, which reduced the energy loss of secondary particles and, therefore, improved the energy resolution.

The charged particles—hydrogen p, d, t, and helium ^{3,4,6}He isotopes produced by absorption in the targets—were detected by two telescopes on the basis of silicon surface–barrier (Si(Au)) and lithium–drift (Si(Li)) detectors. The telescopes with the angle between their axes 180° were placed at a distance of 12 cm from the target. Each telescope included two Si(Au)–s.c.d. with thicknesses of 100 and 450 μm and 14 Si(Li)–s.c.d. each ~3 mm thick [39, 40]. The diameter of the sensitive area of all detectors was 32 mm (the working square—8 cm^2). Si(Au)–s.c.d. operated in the mode of stretching the total depletion detector and therefore, had no sizeable insensitive (dead) regions. The thickness of the dead (lithium) layer Si(Li)–s.c.d. was ~100 μm. Complete measurements of the full thicknesses of detectors were performed by the contact method, while the dead layers Si(Li)–s.c.d. were iden-

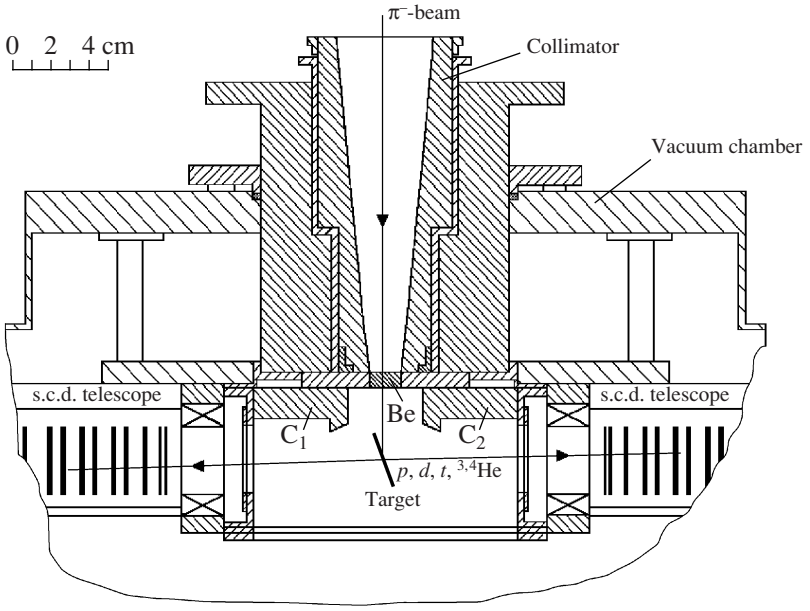

Fig. 1. Layout of two–arm semiconductor spectrometer.

tified by using internal conversion electrons (i.c.e.) from ^{207}Bi source [41]. The full thicknesses of detectors were measured with the uncertainty of 10 microns, while those of the dead layers—5 microns. The deviation from the plane parallel geometry of the detectors was no more than 1%.

An energy resolution of the detectors at room temperature was ~50 keV for α-particles ($E_\alpha \approx 5.5$ MeV) and ~40 keV for internal conversion electrons ($E_e \approx$ 1 MeV). Each detector was placed into the 8-mm-thick-brass mount with the diameter 50 mm.

A total thickness of the sensitive layer of each telescope was ≅43 mm. This value covers the tracks of all charged nuclei produced in absorption reactions on the targets studied. As a result, the high energy resolution was achieved throughout a whole range of measured energies of detected particles.

The identification thresholds were: 3.5 MeV for protons, 4 MeV for deuterons, 4.5 MeV for tritons, and 12 MeV (16 MeV) for helium ions ^{3}He (^{4}He). With the increase of the energy of particles the angular acceptance of each telescope was varied within the following limits: $d\Omega(p)$ = 55–15 msr, $d\Omega(d)$ = 55–17 msr, $d\Omega(t)$ = 55–26 msr. For the short-range helium ions—$d\Omega(^{3,4}\text{He})$ = 55 msr.

2.2. Identification of particles and measurement of their energies. The energy of particles detected by telescopes was determined by summing up energy losses in the telescope detectors. The determination included the energy losses in dead layers of each telescope and target, fixed by the average ionization losses, were accounted for. Since the losses depend on the type of particles, their identification was required already at the step of energy determination.

Issues of particle identification, as well as the problem of rejection of events with the violation of ionization dependence of energy losses resulted from the particle escape out of a detectable volume, edge effects, and nuclear reactions, were solved by the χ^2 method. A detailed description of the application of this criterion to the considered spectrometer is presented in [42].

To gain some insight, the spectrometer capabilities to identify particles are shown in Fig. 2. The measured two-dimensional distribution of energy losses in the second Si(Au)–detector and the first Si(Li)–s.c.d. for particles produced by pion absorption on ^{9}Be target is displayed in Fig. 2a. The proton (p), deuteron (d), triton (t), and helium isotope (^{3,4}He) branches are clearly distinguished. This same data are shown in Fig. 2b after applying the χ^2 method on the hypothesis of stopping in the first Si(Li)–s.c.d. It is clearly seen how the background events, as well as those with particles traversed through Si(Li)–s.c.d., get rejected.

2.3. The spectrometer energy resolution. The principal obstacle to studying the detector's response function is related to obtaining the monoenergetic charged particle beams with the required energy. Using the reaction of pion absorption by nuclei, in this respect, offers some methodical advantages. The momentum of the initial state approaching zero and a sizeable yield of two-particle channels, in which energy release is fixed, makes it possible to obtain monoenergetic particles (p, d, t, and ^{3,4}He) with energies close to the kinematical limits of absorption reaction.

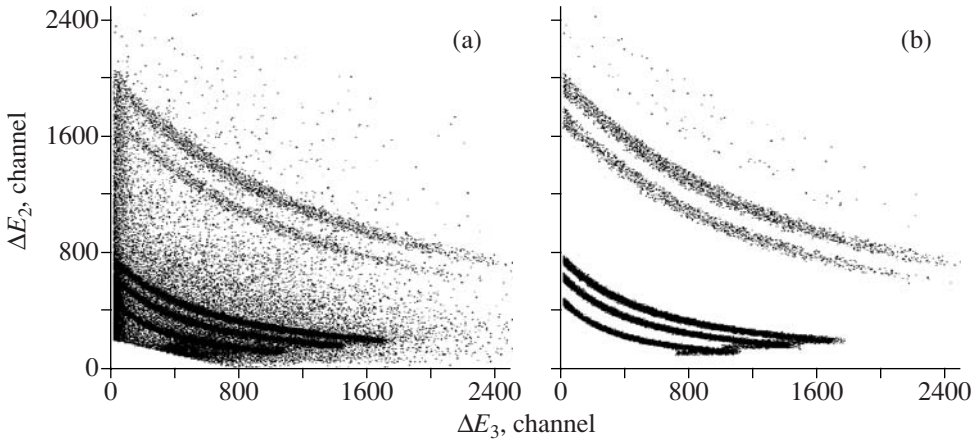

Fig. 2. Two–dimensional distribution of energy released in 2nd identifier Si(Au)–s.c.d. (vertical axis) and 1st Si(Li)–s.c.d. (horizontal axis) for secondary particles from π^--meson caption by ^{9}Be nuclei: (a) before data processing, (b) after data processing.

In the experiment layout considered above the following main factors had an effect on the energy resolution ΔE (FWHM): the uncertainty of energy losses ΔE_{targ} in the target, the fluctuations of energy losses in dead layers of the detector ΔE_{dl}, and the noise of spectrometer electronic channels ΔE_{el} with account for the reverse detector current. Thus, the energy resolution can be represented as follows:

$$\Delta E^2 \approx \Delta E_{\text{targ}}^2 + \Delta E_{\text{dl}}^2 + \Delta E_{\text{el}}^2. \quad (1)$$

The analysis of contributions of different components depending on the type and the energy of detected particles is given in [43].

Aiming at determining the actual spectrometric potential of the spectrometer, the data, obtained in π^--meson absorption reaction by nuclei ^{9}Be and ^{12}C, were used. To measure the energy resolution, the inclusive particle spectra in the following channels were studied:

$$^9\text{Be}(\pi^-, p)X; \quad ^{12}\text{C}(\pi^-, d)X;$$

$$^{12}\text{C}(\pi^-, t)X; \quad ^{12}\text{C}(\pi^-, ^3\text{He})X.$$

Table 3. Experimental (ΔE_{exp}) and calculated (ΔE_{com}) values of energy resolution of s.c.d. telescopes (in keV)

Particle	p	d	t
Energy, MeV	98.5	93.9	84.1
ΔE_{targ}	110	230	230
ΔE_{dl}	306	237	200
ΔE_{el}	327	219	183
ΔE_{com}	462	400	466
ΔE_{exp}	480 ± 25	410 ± 15	480 ± 30

Note: ΔE_{targ}, ΔE_{dl}, ΔE_{el} are computational components of energy resolution.

The measured spectra are shown in Figs. 3 and 4. At the kinematical limits of the reaction one can clearly see sharp peaks resulting from reactions of a two-particle channel, in which the ^{8}He, ^{10}Be, ^{9}Be, and ^{9}Li nuclei are produced in the ground state, respectively. By virtue of the nucleon stability these states have zero width values. Due to the absence of nearby excited levels [38, 44] the widths of the observed peaks permit determining the energy resolution of the spectrometer for detected particles. Note that the inclusive spectra of the deuteron and triton demonstrate a potential of the setup in the spectrometry of excited nuclear states within a sufficiently wide energy range.

For the singly charged particles the experimental values for the resolution ΔE_{exp} (FWHM) are listed in Table 3 [43].

During the measurements with helium ions ^{3,4}He the quantity $\Delta E_{\text{exp}} = 1.9 \pm 0.1$ MeV is considerably larger. Broadening of the instrument line is caused, in general, by the increase of the quantity ΔE_{targ}, which is explained by the increase of ionization losses in the target for doubly charged helium ions.

2.4. Determination of the resolution and absolute spectrometer calibration in measurements of missing mass spectra. In inclusive measurements the resolution of the missing mass (MM) is determined by the uncertainty in the energy measurement of detected particles. The energy released after absorption of stopped pions is much smaller than the energy of the ground state of nuclei produced, therefore, to determine relations between the energy resolution and that in missing mass one can adopt a nonrelativistic approximation. In the case when a particle a, produced in the reaction $\pi^- + A \longrightarrow a + X$, is detected, we have:

$$\Delta E_{MM} \cong \frac{M_A}{M_A - M_a}\Delta E_a, \quad (2)$$

where M_A, m_a denote particle masses.

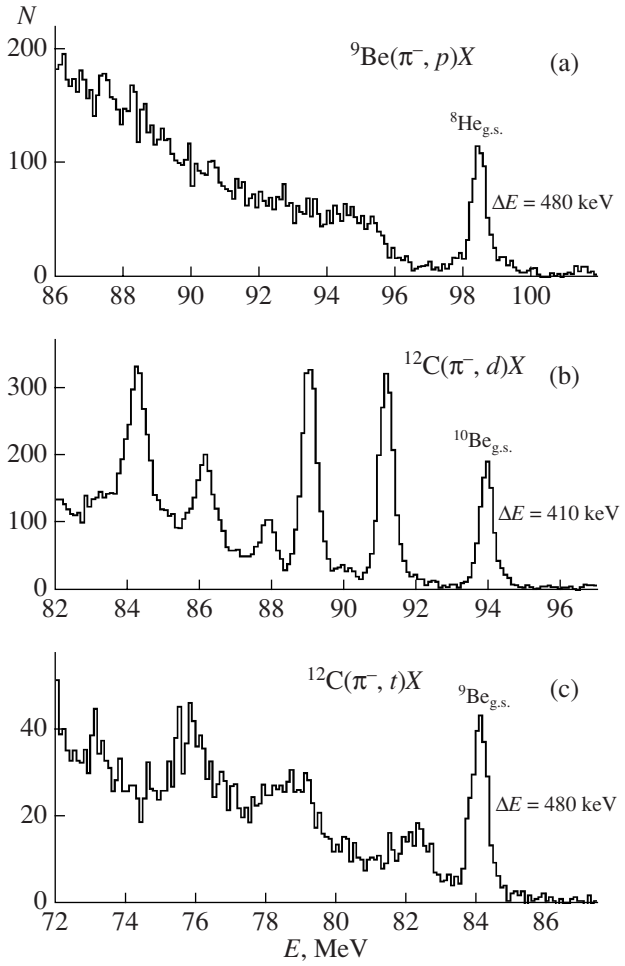

Fig. 3. Inclusive spectra of protons (a), deuterons (b), and tritons (c) from the reaction of π^--meson absorption by nuclei ^{9}Be and ^{12}C.

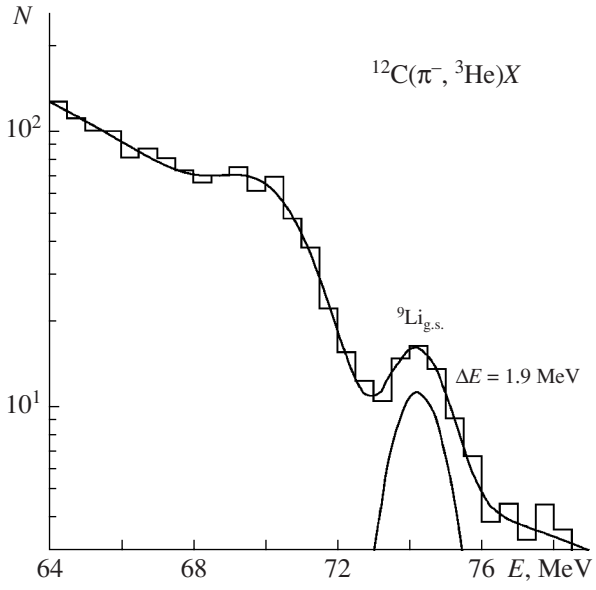

Fig. 4. Inclusive spectrum of ^{3}He ions from the reaction of π^--meson absorption by nuclei ^{12}C. Solid lines—complete description and contribution of two–particle channel ^{12}C(π^-, ^{3}He)^{9}Li.

Thus, for inclusive measurements the resolution of the missing mass depends linearly on the energy resolution. From Table 2 and Eq. (2) it follows that, in measurements carried out with ^{9}Be and ^{11}B targets, the value of the quantity ΔE_{MM} does not exceed 700 keV while detecting singly charged particles, and 3.5 MeV with the registration of helium ions.

In correlation measurements the magnitude of the resolution of the missing mass is determined by three factors: the uncertainties in energy measurements for each particle and those in the particle's opening angle, with the latter originating from an aperture of a finite telescope.

An important advantage of the proposed method for studying the nuclei is connected with the possibility to use, for calibration purposes, results of correlation measurements of charged particles with the known final nuclear states. As an example, let us consider the correlation data obtained with the target ^{12}C. In measurements of the pairs of singly charged particles the following reactions of the three-particle channel can be identified in the spectra of the missing mass:

$$^{12}\mathrm{C}(\pi^-, pp)^{10}\mathrm{Li}, \quad ^{12}\mathrm{C}(\pi^-, pd)^9\mathrm{Li}, \quad ^{12}\mathrm{C}(\pi^-, dd)^8\mathrm{Li},$$
$$^{12}\mathrm{C}(\pi^-, pt)^8\mathrm{Li}, \quad ^{12}\mathrm{C}(\pi^-, dt)^7\mathrm{Li}, \quad ^{12}\mathrm{C}(\pi^-, tt)^6\mathrm{Li}.$$

The ground states of the lithium isotopes produced (except for ^{10}Li) are nucleon–stable thus allowing to use the corresponding missing mass spectra for determining the spectrometer resolution. Just to illustrate this, the spectra for three reactions are shown in Fig. 5. There are sharp peaks corresponding to the ground states of nuclei ^{9}Li, ^{8}Li, ^{6}Li.

The analysis of the results obtained by detecting pairs of singly charged particles demonstrates that the resolution of the missing mass depends weakly on a certain channel of the reaction and in the region close to zero values of *MM* is of the order of ~1 MeV.

The results of measuring the spectra of the missing mass allow also estimating the accuracy of the absolute *MM* energy calibration. For all pairs of detected singly charged particles, except for *pp* pairs, this quantity is $\delta_{MM} \le 0.1$ MeV. When two protons are detected it is $\delta_{MM}(pp) \le 0.2$ MeV. This is due to the strong suppression of the ^{8}He ground state yields in the reaction ^{10}Be(π^-, pp)X, while in the reactions on other targets the states produced are nucleon–unstable ones.

To estimate *MM* resolution in the correlation measurements of helium isotopes ^{3,4}He in coincidence with singly charged particles only the high statistics data, obtained in reactions ^{10}Be(π^-, t^4He)X and ^{12}C(π^-, t^4He)X, were analyzed. The spectra of the missing mass for

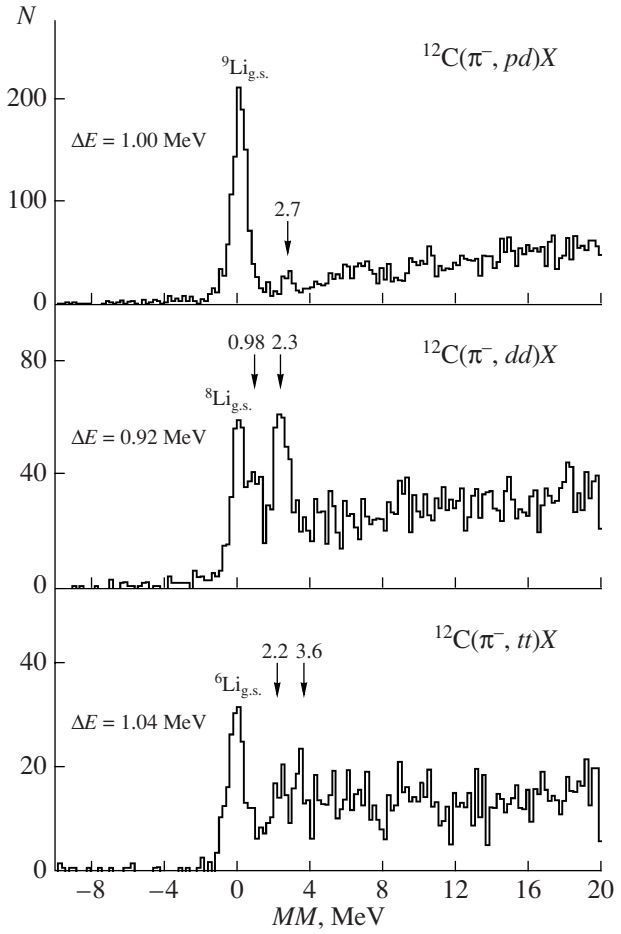

Fig. 5. Missing mass spectra for events (*pd*), (*dd*), and (*tt*) from the reaction of π⁻-meson absorption by nuclei ^{12}C. Numbered arrows denote excited states and point to the corresponding excitation energies.

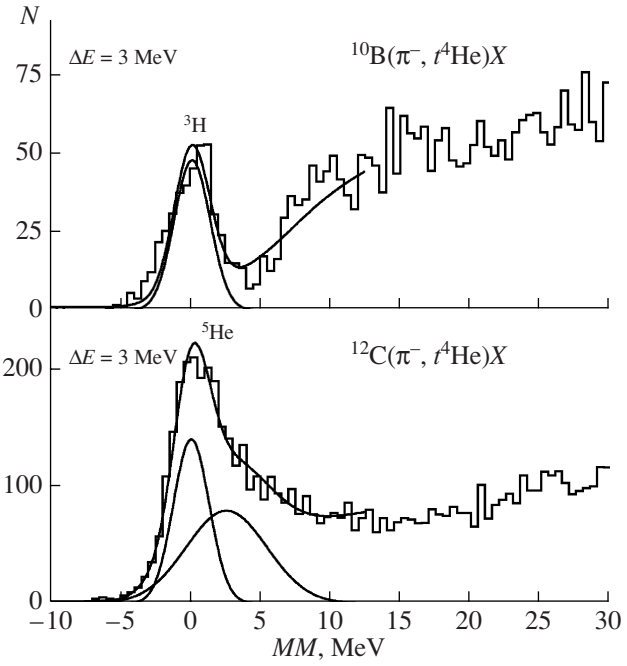

Fig. 6. Missing mass spectra for the reactions ^{10}B(π⁻, t^4He)*X* and ^{12}C(π⁻, t^4He)*X*. Solid lines—complete descriptions and contributions of two–particle channels ^{10}B(π⁻, t^4He)*t*, ^{12}C(π⁻, t^4He)^{5}He(g.s.), and ^{12}C(π⁻, t^4He)^{5}He (E_x = 1.27 MeV).

these reactions are depicted in Fig. 6. The peaks on the plots come from three-particle channels with ^{3}H production, as well as the ground and the first excited states of ^{5}He. Analysis of the results showed that the *MM* energy's resolution in these measurements was 3.0 MeV, whereas the error of absolute energy calibration did not exceed 0.2 MeV.

Thus, the semiconductor setup described above makes it possible to detect long-range charged particles with high energy resolution comparable to that of magnetic spectrometers. Simultaneously it gives us an opportunity to perform correlation measurements of charged particle pairs with a fairly good resolution of the missing mass. It should be noted that the multilayer feature of the spectrometer ensures the measurements to be performed over a wide range in energy and mass without retuning the spectrometer, which is crucial for the rate of collecting statistics and for the minimization of systematic errors.

2.5. Time stability control of spectrometer characteristics. This is accomplished by the analysis of the spectra of the missing mass obtained for different time intervals of data collection.

The energy resolution and the calibration of absolute energy, as well as a probable time variation of these quantities, were controlled by the correlation measurements of *tt* events on the ^{9}Be target. The spectrum of the missing mass, derived from those measurements, is shown in Fig. 7. The peak observed in the region of zero missing mass is related to a three-particle channel of the reaction with triton production. The results obtained for the triton parameters—its mass, which in this case cor-

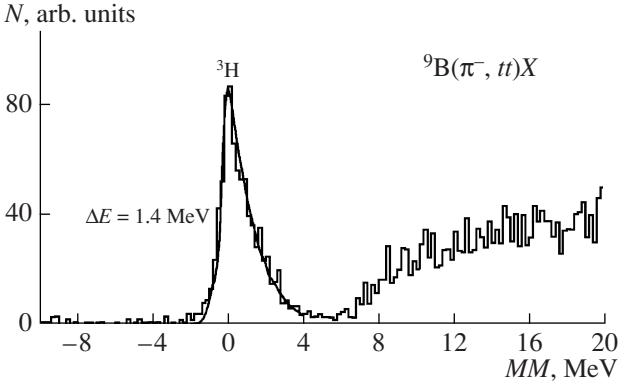

Fig. 7. Missing mass spectrum for the reaction ^{9}Be(π⁻, *tt*)*X*. Solid line—complete description.

responds to the location of the peak $E_{MM} = 0.0 \pm 0.1$ MeV, and the observed width ΔE(FWHM) = 1.4 MeV—prove the correctness of the method and the absence of systematic shifts, and, besides, they are consistent with the data of correlation measurements on ^{11}B and ^{12}C.

It should be noted that some broadening of the triton peak, compared with other calibration peaks (see Fig. 5), results from the angular acceptance of the spectrometer, which leads to broadening of the instrument line with decreasing mass of the undetected residual.

During the work with ^{11}B target the stability of parameters, describing the peak of ^{8}He ground state in the reaction ^{11}B(π^-, *pd*)*X*, was checked (see Fig. 8).

2.6. Determination of possible impurities in targets. A quantitative determination of possible impurities in targets was carried out by identifying the peaks corresponding to the known two-particle reactions on impurity nuclei. It was found [31] that for the target ^{11}B the largest impurity was ^{12}C (8%), whereas a contribution of the remaining (uncontrolled) impurities in the targets ^{11}B and ^{9}Be did not exceed 1%. As is shown below, such a level of impurity in the target ^{11}B does not lead to substantial distortion of the spectra of the missing mass. The method of accounting for impurity contribution is discussed in Chapter 3.

Thus, for all channels with stopped π^--meson absorption, in which superheavy hydrogen isotopes $^{4-7}$H will be studied, the values of the resolution of the missing mass and the calibration error of the absolute are determined. Also, it ought to be noted that all the results, including measurements of the calibration channels of reactions, are obtained within a single experiment, which minimizes potential methodical and systematic errors.

3. RESULTS

3.1. ^{4}H isotope. Experimental investigation of the structure of ^{4}H has been ongoing quite for a while. At the moment it is firmly established that it has no nucleon–stable states. At the same time, the resonance-like states in the continuum were found to exist in a number of experiments. Taking into account excited states of the ^{4}He nucleus it can be noted that the four-nucleon configuration is a qualitatively great advance, as opposed to the case of $A = 3$.

There are two principal approaches to the experimental study of ^{4}H: the measurement of angular distributions in elastic *nt*-scattering and the investigation of the spectrum of the missing mass.

The data of the first of the two approaches is rather limited [45]. As far as we know, the differential cross section of the elastic *nt*-scattering for neutron energy of 1.0, 2.0, 3.5, and 6.0 MeV was measured only in [46]. The analysis of the phase shift of these data was accomplished in [47]. The obtained energy dependencies of the phase shifts $\delta^J_{S,L}$ were described within the framework of single-level Breit-Wigner formalism. The performed analysis showed existence of two levels with $J^P = 2^-$ ($E_r = 3.4$ MeV, $\Gamma = 5.5$ MeV) and $J^P = 1^-$ ($E_r = 5.1$ MeV, $\Gamma = 5.5$ MeV). However, the issue of uniqueness and the accuracy of the description obtained remains open, especially given the fairly large errors in determining the scattering phase shifts [47].

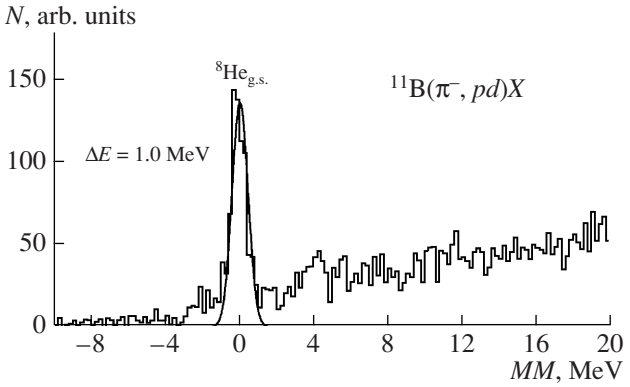

Fig. 8. Missing mass spectrum for the reaction ^{11}B(π^-, *pd*)X. Solid line—contribution of three–particle channel ^{11}B(π^-, *pd*)^{8}He(g.s.).

The experimental data on the charge–conjugate configuration p^3He are known much better [45, 48]. *R*-matrix analysis of the results of the measurements of elastic scattering with this system, which allowed the resonance parameters of the ground and excited states of ^{4}Li to be determined, were carried out in [48]. The transition to ^{4}H was done by charge–conjugating the parameters of ^{4}Li. The resonance parameters of ^{4}H, obtained this way, are shown in Table 4. All the states are *p*-wave resonances. The two more tightly bound states are produced by the valence neutron from the $p_{3/2}$ shell, and two others are generated by the neutron from the $p_{1/2}$ shell.

The issue of uniqueness of the results obtained is still open. As was noted in [49], there is a dependence of the resonance parameters, determined by the *R*-matrix method, on the theory parameters—the channel radii a_c and the quantities B_c, which fix boundary conditions.

Table 4. Energy levels of ^{4}H [45]

E_r, MeV*	J^P	Γ, MeV**
3.19	2^-	5.42
3.50	1^-	6.73
5.27	0^-	8.92
6.02	1^-	12.99

* Resonance energy relative to ^{4}H breakup into triton and neutron.
** Level width.

Table 5. Energy levels of ^{4}H determined by experimental missing mass spectra

Reaction	E_r, MeV*	Γ, MeV**	Reference
^{6}Li(π^-, d)^{4}H	3.3 ± 1.5	<3	[21]
^{7}Li(π^-, t)^{4}H	0.3 ± 1.5	<5	[21]
^{7}Li(π^-, t)^{4}H	2.9 ± 0.5	3.0 ± 1.0	[22]
	6.1 ± 0.5	3.5 ± 1.0	
^{6}Li(^{6}Li, ^{8}B)^{4}H	~3.5	–	[51]
^{7}Li(π^-, t)^{4}H	8 ± 3	<4	[23]
^{7}Li(π^-, t)^{4}H	2.7 ± 0.6	2.3 ± 0.6***	[24]
	5.2	2.3	
^{6}Li(π^-, d)^{4}H	2.7	–	[25]
^{7}Li(^{3}He, ^{3}He^{3}He)^{4}H	2.6 ± 0.2	4.5	[52]
^{9}Be(^{11}B, ^{16}O)^{4}H	3.5	1	[53]
	5.8	2	
^{7}Li(n, α)^{4}H	2.6 ± 0.4	2.1***	[54]
^{9}Be(π^-, dt)^{4}H	3.0 ± 0.2	4.7 ± 1.0	[26]
^{6}Li(π^-, d)^{4}H	3.6 ± 0.6	3.1 ± 0.7	[27]
^{7}Li(π^-, t)^{4}H	3.8 ± 0.3	3.4 ± 0.8	[27]
d(t, p)^{4}H	3.1 ± 0.3	2.3***	[55]
d(^{6}He, α)^{4}H	2.0 ± 0.3	–	[56]
	5.2 ± 0.5	1.2 ± 0.4	
^{6}Li(^{6}Li, ^{8}B)^{4}H	2.3 ± 0.3	–	[56]
^{12}C(^{6}He, nt)X	2.7 ± 0.3	3.3 ± 0.2	[56]
d(t, p)^{4}H	3.05 ± 0.19	4.18 ± 1.02	[58]
t(t, d)^{4}H			
^{9}Be(π^-, dt)^{4}H	1.6 ± 0.1	0.4 ± 0.1***	[13]
	3.4 ± 0.1	0.4 ± 0.1***	
	6.0 ± 0.2	0.5 ± 0.1***	

* Resonance energy relative to ^{4}H breakup into triton and neutron.

** Observed level width.

*** Reduced width.

As a result, the extended R-matrix method was proposed in [49, 50], which makes it possible to determine resonance parameters of the system that are independent of the quantities a_c and B_c. It is important to note that there is a substantial difference in the magnitudes of the resonance parameters obtained by those two methods mentioned above. For example, the resonance parameters ^{5}He (E_r, Γ) for the ground and first excited states, obtained by the standard R-matrix method, are equal to (0.985, 0.963 MeV) and (7.16, 20.61 MeV), respectively, whereas the extended R-matrix method leads to the respective quantities (0.798, 0.648 MeV) and (2.07, 5.57 MeV) [38]. The latter quantities are in better agreement with experimental results on ^{5}He obtained by other methods [38]. In this connection the application of the extended R-matrix method to describe the isotope ^{4}He is highly desirable.

An alternative description of the level structure of ^{4}H rests on the analysis of the spectrum of the missing mass measured in various nuclear processes. The results obtained this way are presented in Table 5. There is a visible discrepancy in the values of resonance parameters of the ^{4}H ground state. The problem of finding the number of ^{4}H resonance states remains unsolved as well.

The search for ^{4}H in the reactions with stopped pion absorption by light nuclei were carried out in a series of papers [21, 22, 23–25, 26, 27, 31]. In earlier experiments the statistics and the angular resolution of measurements were sufficiently low indeed. Also, those experiments suffered background issues.

In the experiments performed at meson factory SIN (nowadays PSI), ^{4}H was detected in the two-particle channels of the reaction of π^--meson absorption by lithium isotopes ^{6,7}Li [24, 25]. As seen from Table 5, the parameters of the ^{4}H ground state for the two reactions coincide within errors. At the same time, note that the indication of a possible excited ^{4}H state in the reaction ^{7}Li(π^-, t)^{4}H, pointed out in the first of these works, was not confirmed in the subsequent publication.

As was mentioned above, the method of investigation of superheavy hydrogen isotopes, presented in this work was first applied in the experiments performed with low energy pion beams at the PNPI synchrophasotron. Within measurement errors the results for the parameters of ^{4}H ground state, obtained in the three-particle channel ^{9}Be(π^-, dt)^{4}H [26], as well as in two-particle channels ^{6}Li(π^-, d)^{4}H and ^{7}Li(π^-, t)^{4}H [27], coincide with each other. It can be noted that the resonance energy in these measurements is somewhat higher with respect to that given in [24, 25].

In the experiment done at LAMPF the search for ^{4}H was carried out in the reaction ^{9}Be(π^-, dt)^{4}H. The resolution of the missing mass and the calibration of the absolute energy in this channel are illustrated by Fig. 9, in which the peaks, corresponding to the ^{6}He production in the ground (nucleon–stable) and first excited states separated by 1.8 MeV, are clearly distinguishable.

The spectrum of the missing mass for the reaction ^{9}Be(π^-, dt)^{4}H is shown in Fig. 10. The sum of triton and neutron masses is taken to be a reference point. In the spectrum depicted in Fig. 10a the peak in the region of small missing masses is clearly visible. This part of the spectrum is represented in Fig. 11 with greater detail. The peak manifests as an apparent structure that hints at the possibility of its formation as a result of superposition of several states.

To resolve these ^{4}H states we used the method of least squares in describing the experimental spectra by the sum of n-particle distributions over phase space ($n \geq 4$) and

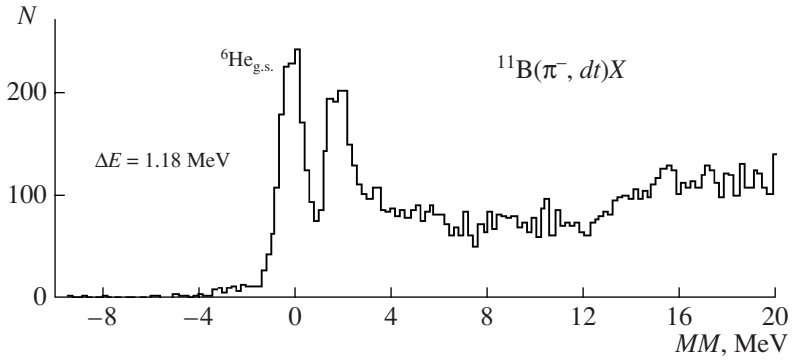

Fig. 9. Missing mass spectrum for the reaction ^{11}B(π^-, dt)X.

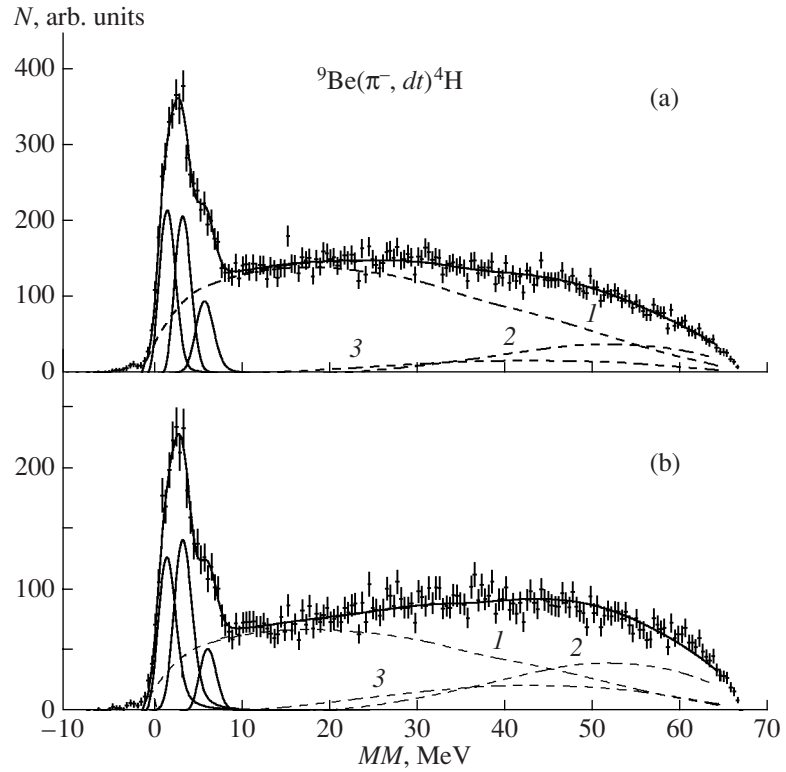

Fig. 10. Missing mass spectra for the reaction ^{9}Be(π^-, dt)X: (a) measured spectrum, (b) measured spectrum with cut $P_x \le 100$ MeV/c imposed. Solid lines—complete descriptions and Breit–Wigner distributions; phase space distributions: *1*, ^{9}Be(π^-, td)tn, *2*, ^{9}Be(π^-, td)$p3n$, *3*, ^{9}Be(π^-, td)$d3n$.

Breit–Wigner distributions. The ^{4}H states were assumed to be p–wave resonances parameterized as in [59]:

$$\frac{dY}{dE} \propto \frac{\Gamma}{(E_\lambda - \Delta_l - E)^2 + (\Gamma/2)^2}, \quad (3)$$

$$\Gamma = 2\gamma^2 P_l(E), \quad (4)$$

$$\Delta_l = \gamma^2 S_l(E), \quad (5)$$

where E_λ is the formal resonance energy, Γ is the resonance width, γ^2 is the reduced width, $S_l(E)$ is the width of the channel phase, $P_l(E)$ is the channel's penetrability function, and E is the energy of the triton's and neutron's relative motion. The resonance energy $E_r = E_l - \Delta_l$. The radius of the channel is chosen to be 4 fm [47].

Several hypotheses concerning the number of ^{4}H states, which contribute to the peak observed, were considered. Firstly, the peak was described by the single excited ^{4}H state. In this case, the parameters of this resonance are $E_r = 3.1 \pm 0.1$ MeV and $\gamma^2 = 3.2 \pm 0.1$ MeV, but this hypothesis must be rejected at the 2% significance level ($\chi^2/N_{DF} = 1.58$ for the number of degrees of

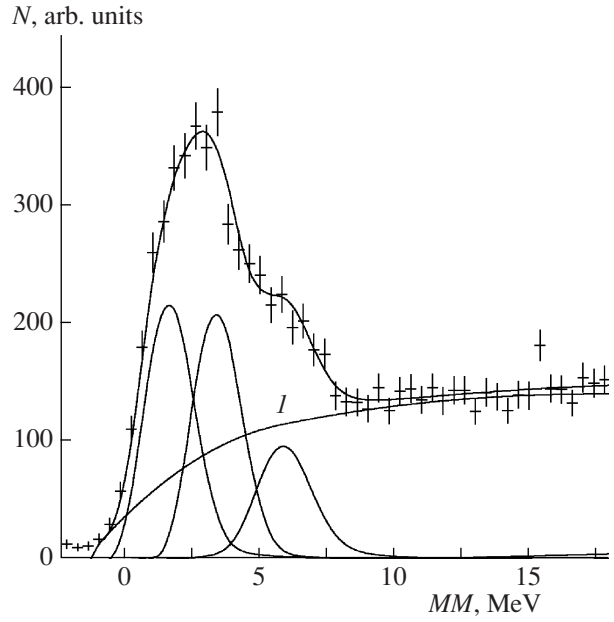

Fig. 11. Fragment of missing mass spectrum for the reaction ^{9}Be(π^-, *td*)*X*. Solid lines—complete description and Breit–Wigner distributions; *1*, phase space distribution ^{9}Be(π^-, *td*)*tn*.

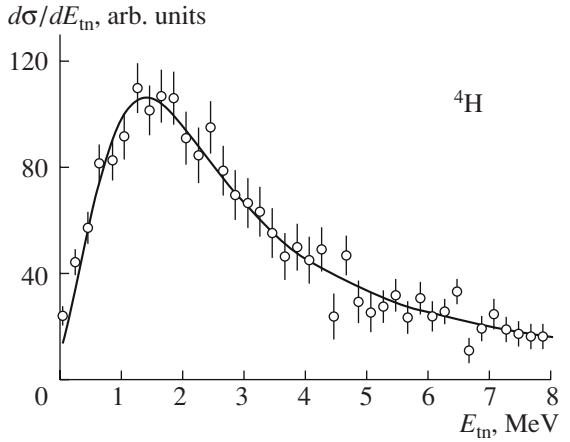

Fig. 12. Energy spectrum of relative motion in system $t + n$, obtained in single–proton knockout reaction in ^{6}He beam with energy of 240 MeV/a.m.u. on a carbon target [57]. Solid line—description of spectrum with account for single resonance ^{4}H state.

freedom $N_{DF} = 32$). Nevertheless, it is important to note that these values for resonance parameters are close enough to those obtained in a large number of works including recent experiments in radioactive beams [57, 58]. A distinctive feature of these works is a description of the experimental spectra with a single resonance state.

A hypothesis of two level ^{4}H ($E_{r1} = 2.4 \pm 0.1$ MeV, $\gamma_1^2 = 1.4 \pm 0.1$ MeV and $E_{r2} = 5.0 \pm 0.2$ MeV, $\gamma_2^2 = 2.6 \pm 0.2$ MeV) can also be rejected at the 2% significance level ($\chi^2/N_{DF} = 1.61$ for $N_{DF} = 29$). Note once again that the obtained values of resonance energies are in good agreement with the results of works [24, 56], in which the two levels were observed.

Satisfactory description of the spectrum ($\chi^2/N_{DF} = 0.88$ for $N_{DF} = 26$) is achieved only by accounting for three ^{4}H states with the following resonance parameters:

$$E_{r1} = 1.6 \pm 0.1 \text{ MeV}, \quad \gamma_1^2 = 0.4 \pm 0.1 \text{ MeV},$$

$$E_{r2} = 3.4 \pm 0.1 \text{ MeV}, \quad \gamma_2^2 = 0.4 \pm 0.1 \text{ MeV},$$

$$E_{13} = 6.0 \pm 0.1 \text{ MeV}, \quad \gamma_3^2 = 0.5 \pm 0.1 \text{ MeV}.$$

The quasifree processes, in which the nucleons of residual nucleus do not directly participate in the reaction, contribute substantially to three-particle channels of the reaction of pion absorption. To enrich the measured spectra with such events and to check for the stability of the results on the level structure of ^{4}H, the momentum of the residual nucleus was constrained ($P_X < 100$ MeV/c). This value certainly does not exceed the expected one for the momentum of the Fermi motion of the intranuclear cluster. Also, such a limitation permits us to considerably suppress a contribution from the final state interactions (FSI) between detected particles and neutrons produced in the reaction [12]. The spectrum of the missing mass obtained in such a manner is depicted in Fig. 10b. It is seen that the peaks related with the resonance states of ^{4}H become more pronounced. Satisfactory description of the spectra is achieved with the same values of resonance parameters as in Fig. 10a.

Thus, our results on ^{4}H do not agree with those by other authors (Table 5), both in the number of observed levels and in the resonance energy of the most bound state. In our opinion, these discrepancies, to a considerable extent, may result from the difference in statistics accumulated. To illustrate this, let us demonstrate in Figs. 12 and 13 the results obtained in recent experiments with radioactive ion beams [57, 58]. In both measurements the experimental spectra are described by a single resonance state. It should be noticed that there seems to be a contradiction between the spectrum given in [57], with the maximum at $E_{MM} = 1.6$ MeV, and the quantity $E_R = 2.7$ MeV. But it is important to observe that both spectra do not contradict an assumption that the observed peak is a result of superposition of several resonance states. It would be highly desirable to obtain experimental information about these reactions with higher statistics.

While considering theoretical predictions concerning the level structure of ^{4}H it should be noted that there are two approaches to the calculation of resonance parameters of nuclear systems in the continuum. In the

first one, the binding energy of the system of four nucleons is calculated, with the existence of the considered resonance postulated. Some of the results [60, 61, 6], obtained in the frames of such an approach, are represented in Table 6, for the earlier references see review [45]. It should be noted that these results do not clarify the experimental situation.

The second approach is to search for the poles of the *S*-matrix on a complex energy plane [62, 9]. As seen from Table 6, the values of resonance parameters, obtained this way, substantially differ from both experimental and other theoretical results. It is observed in [62, 9] that such a difference between two methods is typical of wide resonances.

In [63] the method to relate resonance parameters, obtained by *R*-matrix approach, with *S*-matrix poles, is proposed. This method was used for ^{4}H in [58]. Assuming that only one level is observed in the experiment the authors related the quantities $E_{\text{res}} = 3.05$ MeV and $\gamma^2 = 3.03$ MeV with the pole parameters $E_0 = 1.99$ MeV and $\Gamma = 2.83$ MeV. However, the issue of the correctness of this method applied to the case of several overlapping states is unclear.

So, the experimental status of ^{4}H spectroscopy remains open. Further progress in this field, in our opinion, can be achieved by improving upon statistics in the reactions with radioactive beams.

3.2. ^{5}H isotope. For quite a long time the existence of the ^{5}H isotope was an open question. In [64], the increased proton yield close to the kinematical boundary of the reaction ^{6}Li(π^-, *p*)*X* was observed. However, the interpretation of experimental data turned out to be ambiguous, and perhaps, this increase resulted from the substantial contribution of three-particle channels of the reaction. The up-to-date results with the ^{5}H states observed are given in Table 7.

For the first time, a indication on the ^{5}H existence was obtained in the reactions of stopped π^--meson absorption ^{9}Be(π^-, *pt*)^{5}H in the experiment performed at PNPI [26]. With the assumption that the increase in the spectrum of the missing mass (see Fig. 14) is brought about by a single ^{5}H state, the following values for the resonance parameters were obtained: $E_r = 7.4 \pm 0.7$ MeV, $\Gamma = 8 \pm 3$ MeV (here, E_r is the resonance energy relative to the breakup into a triton and two neutrons). Later on,

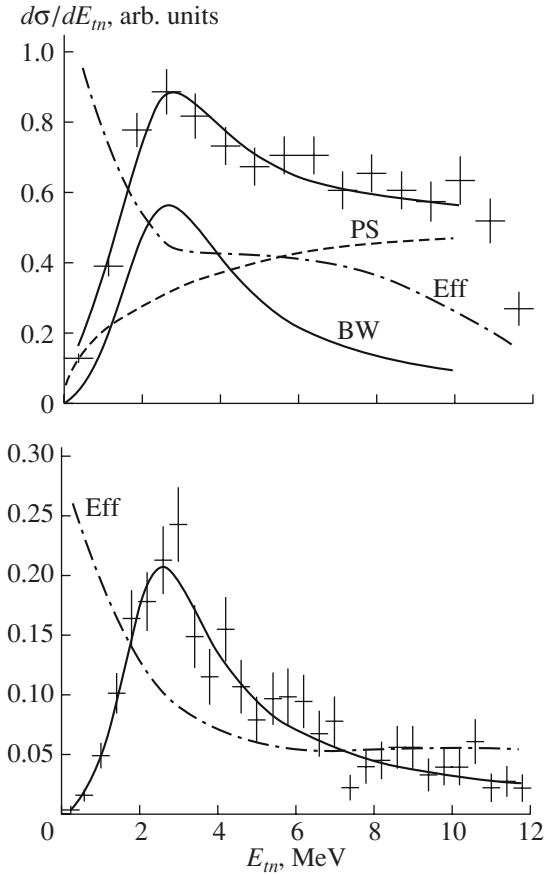

Fig. 13. Energy spectra of ^{4}H [58]. Upper plot—the reaction ^{3}H(*t*, *dn*)*X*, solid line—complete description, dashed line PS—three–particle phase space ($d + t + n$) distribution, dash–dotted line Eff—computed registration efficiency of *dn* events, solid line BW—Breit–Wigner distribution. Lower plot—the reaction ^{2}H(*t*, *pn*)*X*, solid line—complete description, dash–dotted line Eff—computed registration efficiency of *pn* events.

Table 6. Calculated parameters of resonance levels of ^{4}H (in MeV)

J^P	2^-		1^-		0^-		1^-	
Reference	E_r^*	Γ**	E_r	Γ	E_r	Γ	E_r	Γ
[60]	4.7	1.2			6.4	1.8		
[61]	3.2	1.0	4.4	2.3	4.2	2.0	6.4	>5
[6]	2.8							
[62]	1.52	4.11	1.23	5.8	1.19	6.17	1.32	4.72
[9]	1.22	3.34	1.15	3.49	0.77	6.72	1.15	6.38

* Resonance energy relative to ^{4}H breakup into triton and neutron.

** Level width.

Table 7. Experimental parameters of resonance levels of ^{5}H

Reaction	E_r, MeV*	Γ, MeV**	Reference
^{9}Be(π⁻, *pt*)^{5}H	7.4 ± 0.7	8 ± 3	[26]
^{6}Li(π⁻, *p*)^{5}H	11.8 ± 0.7	5.6 ± 0.9	[27]
^{7}Li(π⁻, *d*)^{5}H	9.1 ± 0.7	7.4 ± 0.6	[27]
^{7}Li(^{6}Li, ^{8}B)^{5}H	5.2 ± 0.4	≈4	[65]
p(^{6}He, *pp*)^{5}H	1.7 ± 0.3	1.9 ± 0.4	[66]
t(*t*, *p*)^{5}H	1.8 ± 0.1	≤0.5	[67]
	2.7 ± 0.1	≤0.5	
t(*t*, *p*)^{5}H	≈1.8	≈1.3	[69]
	~5–6		
	~5–6		
^{12}C(^{6}He, 2*nt*)*X*	~3.0	~6.0	[57]
^{9}Be(π⁻, *pt*)^{5}H	5.5 ± 0.2	5.4 ± 0.5	[12]
^{9}Be(π⁻, *dd*)^{5}H	10.6 ± 0.3	6.8 ± 0.5	
	18.5 ± 0.4	4.8 ± 1.3	
	26.7 ± 0.4	3.6 ± 1.3	

* Resonance energy relative to ^{5}H breakup into triton and two neutrons.

** Level width.

indications on the ^{5}H existence were observed in inclusive proton and deuteron spectra in the reactions ^{6}Li(π⁻, *p*)^{5}H and ^{7}Li(π⁻, *d*)^{5}H, respectively [27]. The results of the experiments [26, 27] are close enough to each other; however, statistics of the data of the lithium isotope is essentially lower.

For a long time in the experiments with heavy ion beams the production of ^{5}H isotope was observed only in the reaction ^{7}Li(^{6}Li, ^{8}B)^{5}H, in which the resonance state with $E_r \approx 5.2$ MeV and $\Gamma \approx 4$ MeV was identified [65]. A significant progress in the study of ^{5}H isotope has been made in the experiments using a radioactive ion beam carried out recently at FLNR JINR [66–69] and GSI [57].

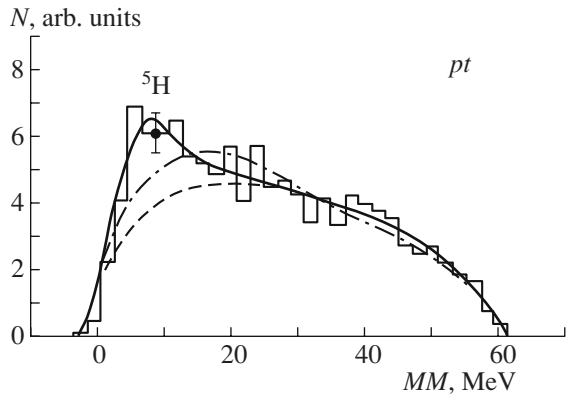

Fig. 14. Missing mass spectrum for the reaction ^{9}Be(π⁻, *pt*)X obtained in the experiment carried out at PNPI [26]. Solid line—description with resonance ^{5}H state included, dashed and dash–dotted lines—versions of description by phase space distribution without inclusion of ^{5}H.

In the reaction of proton knockout, ^{1}H(^{6}He, ^{2}He)*X* at $E(^6\text{He}) = 36$ MeV per nucleon, a narrow level ^{5}H with the resonance energy $E_r = 1.7 \pm 0.3$ MeV and width $\Gamma = 1.9 \pm 0.4$ MeV was observed [66].

The two-nucleon transfer reaction *t*(*t*, *p*)^{5}H at the beam energy $E_t = 57.5$ MeV was explored in [67]. In the events with simultaneous detection of three particles—a proton (outgoing within 18° to 32° relative to the beam direction), a triton, and a neutron—the resonance with $E_r = 1.8 \pm 0.1$ MeV and width $\Gamma < 0.5$ MeV was observed in the spectrum of the missing mass of *tnn* system. Also, in these measurements the existence of the excited state with $E_r = 2.7 \pm 0.1$ MeV and a rather narrow width was hinted at.

The reaction *t*(*t*, *p*)^{5}H was investigated in more detail in [68, 69]. The energy and angular correlations of particles in the breakup of ^{5}H were considered under full kinematical reconstruction of the reaction. Note that unlike in [67], in this work the protons outgoing backwards with respect to the beam direction, were considered. Despite the fact that the spectrum of the missing mass measured in this work has no structural peculiarities, the authors obtained indications of the existence of two levels of ^{5}H with $J^p = 3/2^+$ and $5/2^+$ at $E_r > 2.5$ MeV. These indications are based on the analysis of energy and angular correlations among the fragments of ^{5}H breakup. Lack of clear evidence of the existence of narrow $1/2^+$ ^{5}H level at $E_r \sim 1.8$ MeV the authors explained this by the effects of interference of this state with $3/2^+$ and $5/2^+$ states.

In the experiment performed at GSI [57] the reaction ^{12}C(^{6}He, ^{5}H)*X* at $E(^6\text{He}) = 240$ MeV per nucleon was studied. The tritons and neutrons produced in the reaction were detected in coincidence. The spectrum of the missing mass has a maximum at $E_r \approx 3$ MeV and the width $\Gamma \sim 6$ MeV. Analysis of the angular and energy correlations, in the authors' opinion, hints that this peak is due to the $1/2^+$ ^{5}H state. The authors did not find any evidence of the existence of narrow width resonance levels.

In the experiment carried out at LAMPF the search for ^{5}H was done with several reactions:

$$^9\text{Be}(\pi^-, pt)^5\text{H}, \quad ^9\text{Be}(\pi^-, dd)^5\text{H}, \quad ^9\text{Be}(\pi^-, ^4\text{He})^5\text{H}.$$

In Figs. 15 and 16 the spectra of the missing mass for the reactions ^{9}Be(π⁻, *pt*)*X* and ^{9}Be(π⁻, *dd*)*X* are displayed. The sum of the masses of a triton and two neutrons is taken to be a reference point. It is seen that the distributions of the phase space do not allow the experimental spectra to be described. The structures observed in the spectra are due to three-particle channels of the reaction with production of ^{5}H isotope in the ground and excited states. Description of the spectra

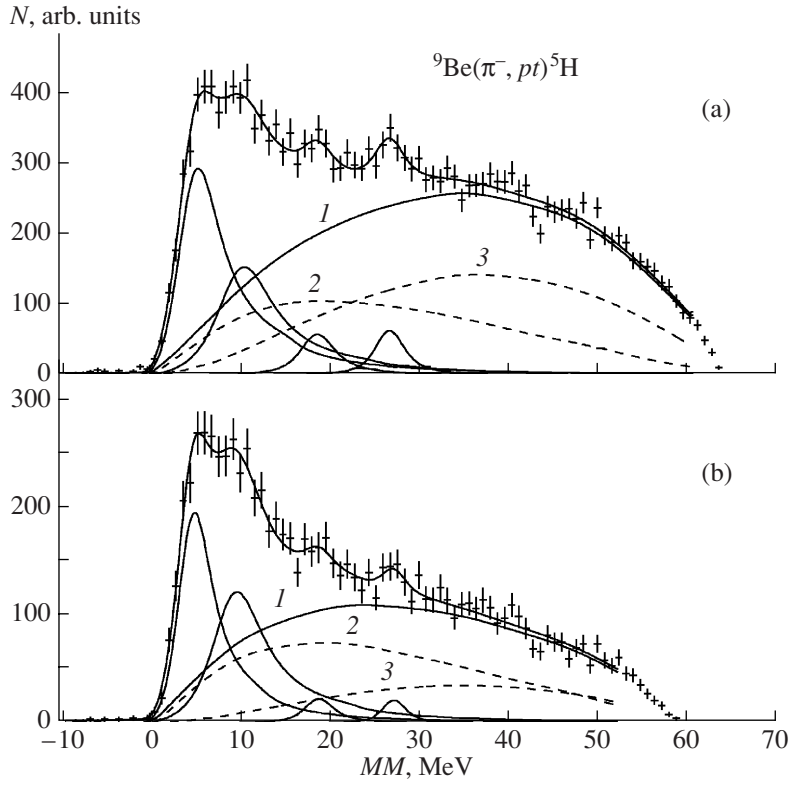

Fig. 15. Missing mass spectra for the reaction ^{9}Be(π^-, *pt*)*X*: (a) measured spectrum, (b) measured spectrum with the cut imposed on the momentum of undetected residual $P_x \le 100$ MeV/*c*. Solid lines—complete description and Breit–Wigner distributions; phase space distributions: *1*, total distribution, *2*, ^{9}Be(π^-, *pt*)^4*Hn*, *3*, ^{9}Be(π^-, *pt*)*t*2*n*.

was carried out by analogy to the case of ^{4}H (see Section 3.1).

To describe ^{5}H states the Breit–Wigner formula was used. Such a choice is related to the lack of reliable theoretical models to describe resonance states of this isotope. Therefore, this rough approximation should only be considered as a convenient way of representing experimental information, which provides the opportunity to compare with other experimental data.

The spectrum of the missing mass for the reaction ^{9}Be(π^-, *pt*)*X* (Fig. 15a) and ^{9}Be(π^-, *dd*)^{5}H (Fig. 16a) can be described using four states of the ^{5}H isotope (the values χ^2/N_{DF} are 1.05 and 0.94, respectively). The values of the resonance states are shown in Table 8. It should be noted that satisfactory description of experimental data cannot be achieved unless multiparticle channels with creation of the singlet neutron pair ^2n or ^{4}H in the final state are taken into account. It is important to underline that the shapes of spectra shown in Figs. 15a and 16a substantially differ. The yields of the same ^{5}H states in the channels with *pt* and *dd* pairs detected differ as well. This can indicate a difference in

Table 8. Resonance parameters for ^{5}H isotope obtained in stopped pion absorption by nuclei ^{9}Be

Reaction channel				Weighted mean values	
^{9}Be(π^-, *pt*)^{5}H		^{9}Be(π^-, *dd*)^{5}H			
E_r, MeV*	Γ, MeV**	E_r, MeV	Γ, MeV	E_r, MeV	Γ, MeV
5.2 ± 0.3	5.5 ± 0.5	6.1 ± 0.4	4.5 ± 1.2	5.5 ± 0.2	5.4 ± 0.5
10.4 ± 0.3	7.4 ± 0.6	11.4 ± 0.7	5 ± 1	10.6 ± 0.3	6.8 ± 0.5
18.7 ± 0.5	3.9 ± 2.0	18.3 ± 0.5	5.5 ± 1.7	18.5 ± 0.4	4.8 ± 1.3
26.8 ± 0.4	3.0 ± 1.4	26.5 ± 1.0	6 ± 3	26.7 ± 0.4	3.6 ± 1.3

* Resonance energy relative to ^{5}H breakup into triton and two neutrons.

** Level width.

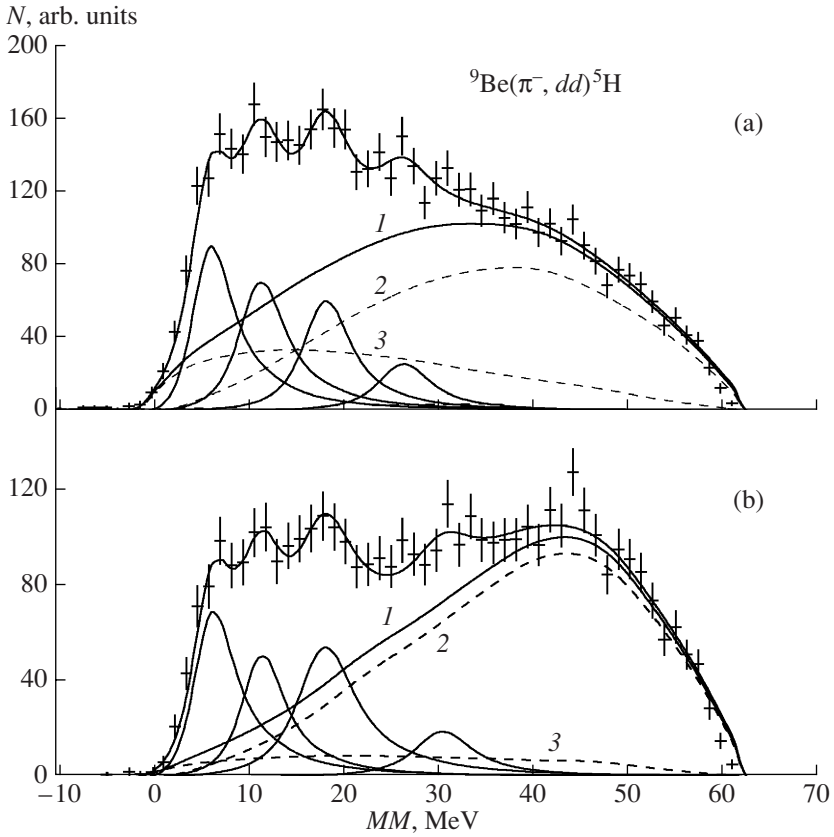

Fig. 16. Missing mass spectra for the reaction ^{9}Be(π$^-$, dd)X: (a) measured spectrum, (b) measured spectrum with the cut imposed on the momentum of undetected residual $P_x \le 100$ MeV/c. Solid lines—complete description and Breit–Wigner distributions; phase space distributions: *1*, total distribution, *2*, ^{9}Be(π$^-$, dd)t2n, *3*, ^{9}Be(π$^-$, pt)^{4}Hn.

the mechanism of channel formation. In [7] it was supposed that the observed parameters of wide resonance states may strongly depend on the reaction mechanism. However, as seen from Table 8, in our case the parameters of ^{5}H states lie well within experimental errors.

In Figs. 15b and 16b the spectra of the missing mass for the reactions ^{9}Be(π$^-$, pt)X and ^{9}Be(π$^-$, dd)^{5}H, with the cut on the momentum of residual nucleus $P_X <$ 100 MeV/c, are depicted. As has been mentioned above, such a limitation allows us to enrich the spectra by events with quasifree pion absorption and to considerably suppress the contribution coming from FSI. The spectra were described with parameter values of Breit–Wigner distributions given in Table 8. The values obtained $\chi^2/N_{DF} = 1.2$ for pt events and 1.1 for dd events do not contradict the hypothesis of existence of the four ^{5}H isotope resonance states.

Two highly excited states ($E_r = 18.5$ and 26.8 MeV) are less noticeable. In this connection, we used the χ^2 criterion to check for hypotheses according to which the spectra were described by three resonance states, successively excluding the levels with E_r = 18.5 and 26.7 MeV. Both hypotheses can be rejected at the 10% significance level.

It should be noted that the obtained results for the channel ^{9}Be(π$^-$, pt)^{5}H do not contradict earlier measurements presented in [26], where due to a worse energy resolution and lack of statistics the first two levels of ^{5}H could not be separated.

The search for the ^{5}H isotope was conducted in the two-particle channel of the absorption reaction ^{9}Be(π$^-$, ^{4}He)X as well. The spectrum of the missing mass obtained for this reaction is shown in Fig. 17. The search for effects indicating the two-particle channel's production of ^{5}H was done as follows. The region of spectrum corresponding to highly excited states of the residual system was described by the sum of phase spaces of every possible channel of the reaction but the two-particle ones. At that, the possibility to produce singlet neutron pairs, as well as a contribution of the channel with ^{4}H, was taken into account.

Let us mention that the experimental spectra are fairly well described by a total distribution of the phase space ($\chi^2/N_{DF} = 1.2$). The structural peculiarities of the spectrum, which would indicate the existence of ^{5}H resonance, were not revealed.

A possible explanation of the absence of ^{5}H production in the two-particle channel of the reaction can be related to the structure of this isotope. In the correlation measurements we found that widths of the observed ^{5}H levels were highly large. Consequently, the lifetimes of these states are short and become comparable to the duration of the reaction. In such a situation the probability of the ^{5}H production is larger for those channels in which nucleons, which constitute the ^{5}H state, do not directly participate in the reaction, and this configuration largely overlaps with the wave function of nucleons in the initial nucleus. In the case of ^{5}H produced in the two-particle channel of the reaction ^{9}Be(π^-, ^{4}He)^{5}H the momentum of the formed atomic state will be ~700 MeV/c. Such large values are strongly suppressed in the momentum distribution related to Fermi motion of intranuclear cluster. Besides, taking into account the pion's negative charge and α-cluster structure of ^{9}Be it should be supposed that the production of fast ^{4}He demands for the mechanisms to involve the nucleons of the residual nucleus into the absorption process. Hence, a conclusion can be drawn that quasifree processes cannot lead to the ^{5}H production in the two-particle channel of the reaction.

The results of the theoretical calculations performed so far are presented in Table 9.

The difference in theoretical approaches ought to be pointed out while analyzing the results obtained. In [5, 6, 70] the binding energy of the corresponding states was calculated. In [71, 72] the energy dependence of the corresponding phase shifts was determined. Lastly, in [9, 73] the parameters of resonance states were fixed by the poles of S-matrix. It is seen from Table 8 that, as in the case of ^{4}H, the latter approach leads to noticeably lower values of resonance energies. However, the issue of how to compare these calculable quantities with experimental data remains open.

By comparing experimental (Table 8) and theoretical (Table 9) results on the level structure of ^{5}H one can draw a conclusion that there is a considerable discrepancy in the data. The results for the lowest lying state, obtained in the reaction of stopped pion absorption, most closely match the experimental data of [65] and theoretical calculations in [5, 70]. At the same time, the results of other works are 2–4 MeV lower. One of the possible explanations can be related to the suppression of $J^p = 1/2^+$ state production in the reaction of stopped pion absorption.

The important result of our measurements is the observation of few excited levels of the ^{5}H isotope. It should be noted that the resonance energies of these states exceed the threshold of ^{5}H breakup into five free nucleons.

3.3. ^{6}H isotope. An evidence for the existence of the ^{6}H isotope was for the first time obtained in two reactions with heavy ions. In the first one, ^{7}Li(^{7}Li, ^{8}B)X at

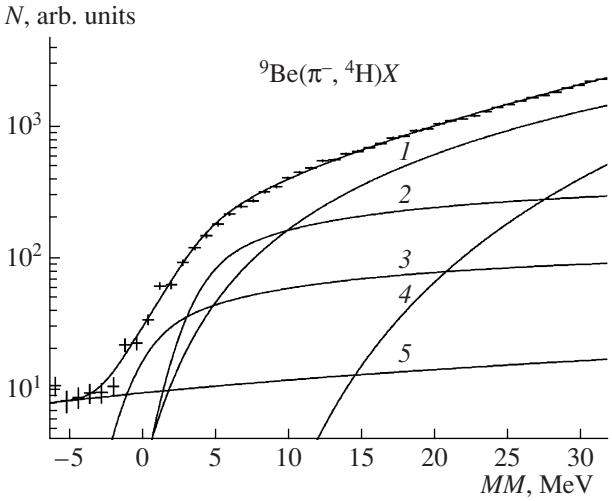

Fig. 17. Missing mass spectrum for the reaction ^{9}Be(π^-, ^{4}He)X. Solid lines—complete description; phase space distributions: *1*, ^{9}Be(π^-, ^{4}He)2nt, *2*, ^{9}Be(π^-, ^{4}He)n^4H, *3*, ^{9}Be(π^-, ^{4}He)^2nt, *4*, ^{9}Be(π^-, ^{4}He)3nd, *5*, background distribution.

^{7}Li with an ion beam energy of 82 MeV, the resonance state of ^{6}H nucleus with $E_r = 2.7 \pm 0.4$ MeV, $\Gamma = 1.8 \pm 0.5$ MeV (E_r is the resonance energy relative to the breakup into a triton and three neutrons) was observed [73]. The second reaction, ^{9}Be(^{11}B, ^{14}O)X at the energy $E(^{11}\text{B}) = 88$ MeV (Fig. 19), was studied in [74], where the authors also obtained the results indicating the formation of ^{6}H state with $E_r = 2.6 \pm 0.5$ MeV, $\Gamma = 1.3 \pm 0.5$ MeV.

The parameters listed above agree with each other, but in both works statistics were rather low. Furthermore, in [73] a considerable contribution to the spectrum coming from impurities in the target was observed. The ^{6}H isotope was not detected in the reac-

Table 9. Calculated parameters of ^{5}H isotope (in MeV)

J^P	$1/2^+$		$3/2^+$		$5/2^+$	
reference	E_r^*	Γ**	E_r	Γ	E_r	Γ
[5]					6	~6
[70]	~6	>4				
[71]	~2.7	~3	~6.6	~8	~4.8	~5
[72]	~3	1–4				
[6]	~2					
[73]	1.6	2.5	3	4.8	2.9	4.1
[9]	1.6	1.5	3.2	3.9	2.8	2.5

* Resonance energy relative to ^{5}H breakup into triton and two neutrons.

** Level width.

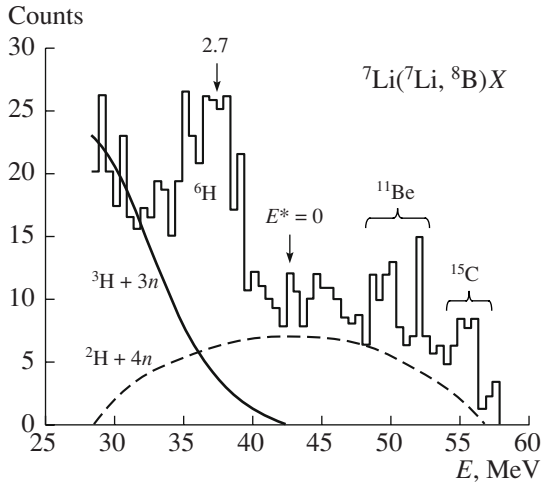

Fig. 18. Energy distribution of ^{8}B ions [73]. Solid line—distribution over five–particle phase space, dashed line—background distribution. Arrows point to the threshold of the reaction and a location of the resonance ^{6}H state.

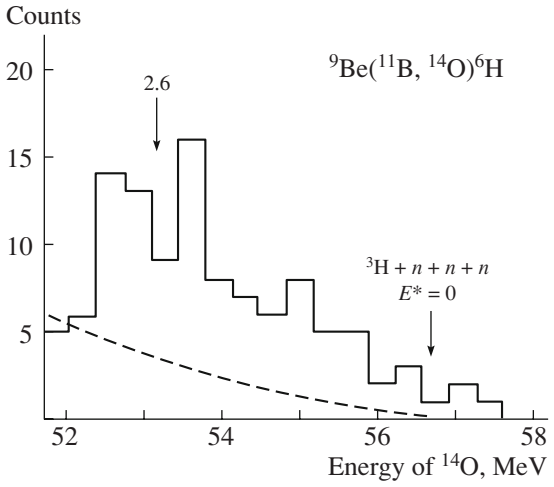

Fig. 19. Energy distribution of ^{14}O ions [73]. Solid line—distribution over five–particle phase space, dashed line—background distribution. Arrows point to the threshold of the reaction and a location of the resonance ^{6}H state.

tion of the double charge exchange ^{6}Li(π^-, π^+)X at E_π = 220 MeV [75].

In the earlier investigations of the reactions of stopped pion absorption the signs of ^{6}H production in the two channels of the reaction—^{9}Be(π^-, pd)X [26] and ^{7}Li(π^-, p)X [27]—were not seen as well.

The theoretical description of the ^{6}H nuclear state is a rather difficult problem. The methods of describing three-particle states near the drip line (in Section 3.2 the works, in which these methods were applied to the case of ^{5}H, are cited) developed recently are inapplicable in the case of ^{6}H, whose ground state can presumably be represented as $t + n + n + n$. An attempt to describe ^{6}H by other methods faces formidable computational obstacles [6]. We mention only the work [5], in which calculations, performed by the method of angular potential functions predict the existence of the ground state ^{6}H ($J^\pi = 2^-$) with E_r = 6.3 MeV.

Table 10. Resonance parameters for ^{6}H isotope

Reaction channel			
^{9}Be(π^-, pd)^{6}H		^{11}B(π^-, p^4He)^{6}H	
E_r, MeV*	Γ, MeV**	E_r, MeV	Γ, MeV
6.6 ± 0.7	5.5 ± 2.0	7.3 ± 1.0	5.8 ± 2.0
10.7 ± 0.7	4 ± 2	–	–
15.3 ± 0.7	3 ± 2	14.5 ± 1.0	5.5 ± 2.0
21.3 ± 0.4	3.5 ± 1.0	22.0 ± 1.0	5.5 ± 2.0

* Resonance energy relative to ^{5}H breakup into triton and three neutrons.

** Level width.

In the experiment carried out at LAMPF the search for ^{5}H was done with several channels of the reactions:

$$^9\text{Be}(\pi^-, pd)^6\text{H}, \quad ^{11}\text{B}(\pi^-, p^4\text{He})^6\text{H},$$

$$^{11}\text{B}(\pi^-, d^3\text{He})^6\text{H}, \quad ^9\text{Be}(\pi^-, ^3\text{He})^6\text{H}.$$

In Fig. 20 the spectrum of the missing mass for the reaction ^{9}Be(π^-, pd)X is presented. First of all, note that there is no indication of the existence of ^{6}H bound states in the region of negative MM values. A low background in this region results from random coincidences in correlation measurements. At the same time, in the region $MM > 0$ there are structures in the spectrum that can be caused by the production of ^{6}H resonance states. The procedure of identification of these states and determination of their parameters is analogous to that in the case of ^{4}H and ^{5}H isotopes. Note that in describing the experimental spectrum, in addition to the channels of the reaction with creation of singlet pairs of neutrons ^2n and ^{4}H, the contribution from the channel with ^{5}H production was also taken into account.

As seen from Fig. 20a the distributions of the phase space cannot reproduce the observed structure for $MM < 25$ MeV. Note that the leading contribution to the total distribution comes from five-particle phase spaces with a dineutron in the final state ($d + p + {}^2n + t + n$).

Satisfactory description ($\chi^2/N_{DF} = 0.95$) of the spectrum is achieved only with four ^{6}H states included. These states were described by the simple Breit–Wigner formula, in which the level width Γ was taken to be constant. The parameters of resonance ^{6}H states are given in Table 10. It should be noted that, as in the case of ^{5}H, the validity limits of using the superposition of Breit–Wigner distributions in describing the observed structure remain undetermined.

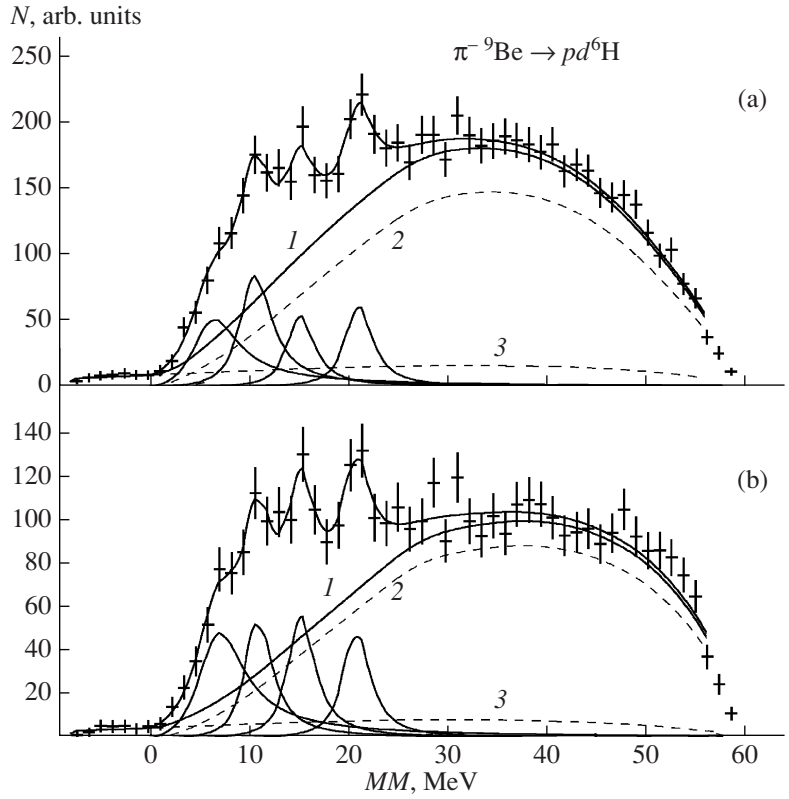

Fig. 20. Missing mass spectra for the reaction ^{9}Be(π^-, *pd*)X: (a) measured spectrum, (b) measured spectrum with the cut imposed on the momentum of undetected residual $P_x \le 100$ MeV/*c*. Solid lines—complete description and Breit–Wigner distributions: *1*, total distribution over phase space; dashed lines: *2*, four–particle distribution over phase space, *3*, background coming from random coincidences.

The spectrum obtained with the cut imposed on the momentum of undetected residual $P_X \le 100$ MeV/*c* is shown in Fig. 20b. Such a restriction permits us to suppress FSI between the detected particle and one of the neutrons produced, and also to enrich the spectrum with events related to processes of quasifree absorption. Description of the spectrum with parameters of Breit–Wigner distributions, given in Table 10, led to the value $\chi^2/N_{DF} = 1.01$, which confirmed the hypothesis of the possible existence of four resonance states of the ^{6}H isotope.

A comparison with our earlier searches for ^{6}H in the reactions ^{9}Be(π^-, *pd*)*X* [26] shows that in the experiment performed at PNPI statistics and the resolution of the missing mass were insufficient to correctly describe the spectrum.

In measurements with the target ^{11}B the production of ^{6}H can be observed in the spectra of the missing mass of two channels of the reactions ^{11}Be(π^-, p^4He)*X* (Fig. 21) and ^{11}Be(π^-, d^3He)*X* (Fig. 22). The target ^{11}B contains impurity ^{12}C, therefore, the corresponding contribution coming from the reactions ^{12}C(π^-, p^4He)*X* and ^{12}C(π^-, d^3He)*X* was subtracted from the measured spectra (Figs. 21a and 22a). The contribution of these spectra (Figs. 21b and 22b) has been determined with the help of normalization of the spectra measured with the ^{12}C target in the same run to a relative portion of impurity (8%). The spectra obtained this way are depicted in Figs. 21c and 22c.

The analysis of spectra obtained with ^{11}B was carried out in two ways. First, the values of parameters of resonance ^{6}H states obtained with ^{9}Be were used to describe the spectra. In this case, the values χ^2/N_{DF} turned out to be 0.88 and 0.97 for the reactions ^{11}B(π^-, p^4He)*X* and ^{11}B(π^-, d^3He)*X*, respectively, which does not contradict the hypothesis of the existence of four levels of the ^{6}H isotope. Then, the location, the level widths, and also the number of levels, were treated as free parameters in describing the spectra. In this case, acceptable description of the spectrum ($\chi^2/N_{DF} = 0.87$) for the reaction ^{11}B(π^-, p^4He)*X* (Fig. 22c) is achieved by including only three resonance states with parameters as given in Table 10. Notice that, within experimental errors, the values of these parameters coincide with the results obtained in the reaction ^{9}Be(π^-, *pd*)*X*. Description of the spectrum in the reaction ^{11}B(π^-, d^3He)*X* (Fig. 22c) is possible without referring to ^{6}H, but satisfactory value $\chi^2/N_{DF} \approx 1$ is achieved only by including

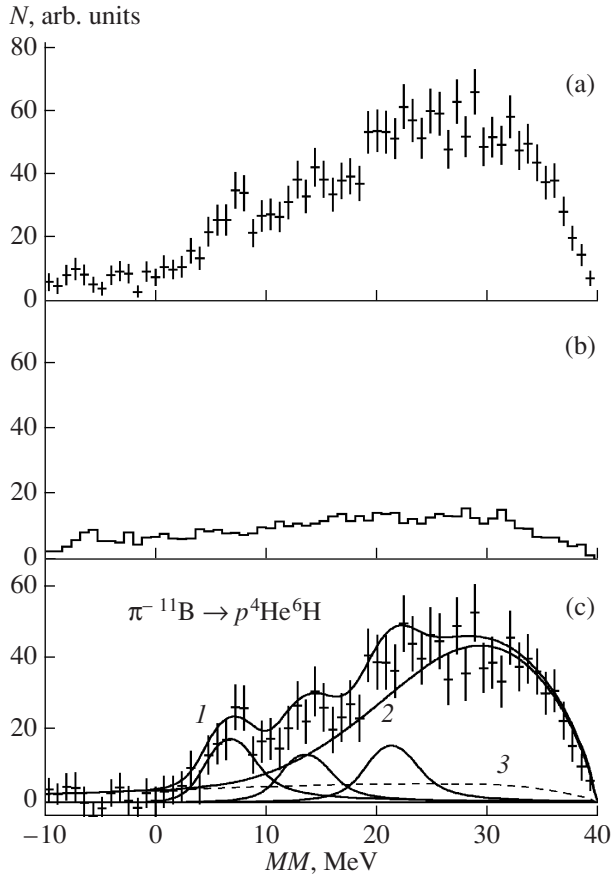

Fig. 21. Missing mass spectra for the reaction ^{11}Be(π^-, p^4He)X: (a) spectrum on the target ^{11}B, (b) spectrum for the reaction ^{12}C(π^-, p^4He)X normalized to amount of ^{12}C impurity in ^{11}B target, (c) spectrum after removing contribution from impurity. Solid lines—Breit–Wigner distributions: *1*, complete description, *2*, total distribution over phase space. Dashed line *3*, background coming from random coincidences.

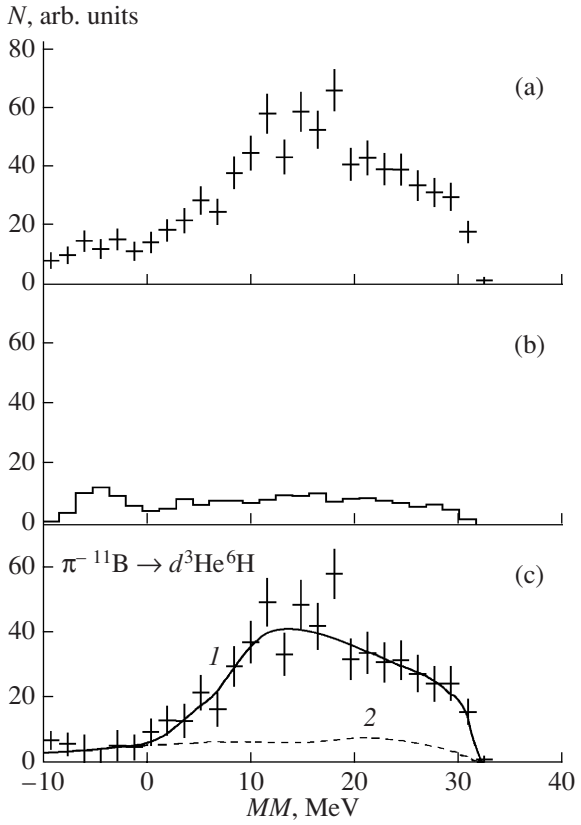

Fig. 22. Missing mass spectra for the reaction ^{11}Be(π^-, d^3He)X: (a) measured spectrum on the target ^{11}B, (b) measured spectrum for the reaction ^{12}C(π^-, d^3He)X normalized to amount of ^{12}C impurity in ^{11}B target, (c) spectrum after removing contribution from impurity, *1*, complete description, *2*, background coming from random coincidences.

the channel with production of superheavy hydrogen isotope ^{5}H (^{3}He + d + n + ^{5}H) into the total spectrum of phase space. It should be noted that statistics of the data with detection of the d^3He pair is very low.

The given analysis showed no contradiction in the results obtained with two targets. However, in comparison with measurements with ^{9}Be, the energy resolution and statistics of the data, obtained with ^{11}Be, are worse, which hamper observation of ^{6}H states. Hence, the assumption that the data obtained in the reaction ^{9}Be(π^-, pd)X is more adequate in reproducing the level structure of the ^{6}H isotope.

The value of the resonance energy of the lowest lying state of the ^{6}H isotope given in Table 10 is located considerably higher than the one obtained from earlier experiments [18, 19]. At that, it should be underlined that statistics of our data is more than an order of magnitude higher. Besides, a wide range of missing mass measured in the experiment minimizes the influence of the effects of phase space on the results; in particular, this conclusion is illustrated by spectra obtained with the cut imposed on residual momentum. However, one cannot exclude the possibility of discrepancy coming from the nuclear structure of the targets ^{9}Be and ^{11}B.

Our result agrees with theoretical predictions given in [5].

An important result of our measurements is the observation of a few excited states of ^{6}H isotope. As in the case of ^{5}H, the resonance energies of excited ^{6}H states exceed the threshold of isotope breakup into free nucleons. Excitations of this system of free nucleons turn out to be rather high and reach the value ~13 MeV (or 2.2 MeV per nucleon).

Additional confirmation of the existence of ^{6}H isotope levels with E_r = 10.7 and 15.3 MeV can be gained from the spectroscopy data of ^{6}He isotope [52]. In the spectrum of the missing mass measured in the reaction ^{7}Li(^{3}He, p^3He)X at $E(^3\text{He})$ = 120 MeV, the two relatively narrow states ($\Gamma \le 2$ MeV) of ^{6}He with excitation

energies $E_x \approx 32.0$ and 35.7 MeV were observed. Converting these values into the binding energies of the corresponding states (the quantity B is positive for bound systems) we obtain $B(^6\mathrm{H}) = -2.2 \pm 0.7$ and -6.8 ± 0.7 MeV, $B(^6\mathrm{He}) = -2.7$ and -6.4 MeV, respectively. The Coulomb energy of ^{6}He does not exceed 0.7 MeV [1], therefore, it is reasonable to suppose that observed levels are likely to be isobaric analog states for ^{6}H.

The search for ^{6}H formation was also performed in the two-particle channel of the absorption reaction $^9\mathrm{Be}(\pi^-, {}^3\mathrm{He})X$.

The spectrum of the missing mass of the reaction $^9\mathrm{Be}(\pi^-, {}^3\mathrm{He})X$ is displayed in Fig. 23a. The search for effects of ^{6}H production in the two-particle channel of the reaction was carried out in a manner similar to the case of ^{5}H (Section 3.2).

As seen from Fig. 23a, a good description of experimental spectrum ($\chi^2/N_{DF} = 1.2$) is achieved with the total distribution over the phase space without bringing in the two-particle channel. There are no structural peculiarities in the spectrum indicating the presence of ^{6}H resonance.

In the process of stopped pion absorption the leading contribution to ^{3}He formation comes from secondary processes taking place at the cascade stage of the reaction [54]. A two-arm spectrometer enables us, on the one hand, to suppress the contribution of such processes, and on the other hand, to make use of kinematical features of the two-particle channel of the reaction. In the reaction $\pi^- + {}^9\mathrm{Be} \longrightarrow {}^3\mathrm{He} + {}^6\mathrm{H} \longrightarrow {}^3\mathrm{He} + t + 3n$ the triton produced goes out preferably backward to the direction of outgoing ^{3}He. Therefore, in measurements of ^{3}He, when the opposite telescope detects a triton, relative enrichment of the energy spectrum can occur due to the contribution of the two-particle channel. The spectrum obtained is shown in Fig. 23b. It is seen that once again there are not any indications of ^{6}H formation.

A possible explanation of the absence of ^{6}H formation in the two-particle channel of the reaction is similar to the case of ^{5}H: quasifree processes cannot lead to the latter.

Thus, a joint analysis of the spectra of the missing mass in the reactions $^9\mathrm{Be}(\pi^-, pd)X$ and $^{11}\mathrm{Be}(\pi^-, p^4\mathrm{He})X$ let, for the first time, separate the structures in the excitation spectra of the system $t + 3n$, which point to the existence of four levels of ^{6}H. Furthermore, evidences for on the existence of three excited states ($E_r > 10$ MeV) were as well obtained for the first time. It should be noted that the spectrum shape and the ratios of resonance branching are clearly different for the reactions $^9\mathrm{Be}(\pi^-, pd)X$ and $^{11}\mathrm{Be}(\pi^-, p^4\mathrm{He})X$. Presumably, this points to different mechanisms of origin of these channels. Nonetheless, the values of distribution parameters for both channels are found to be well within measurement errors, thus demonstrating reliability of the results. At the same time it should be noted that complexity of the problem to describe structures caused by wide overlapping levels seems to demand for higher statistics of the reactions under study.

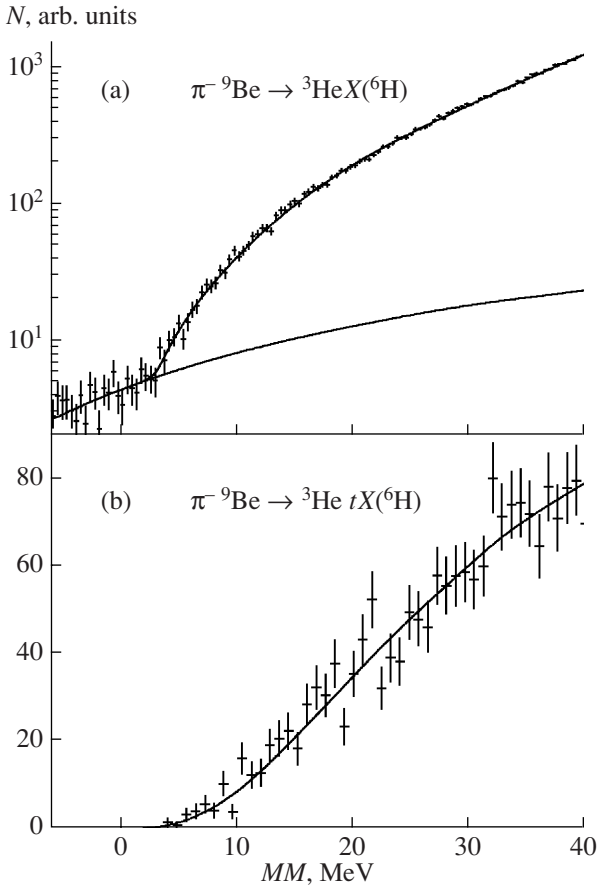

Fig. 23. Missing mass spectra for the reaction $^9\mathrm{Be}(\pi^-, {}^3\mathrm{He})X$: (a) total experimental spectrum (solid line—complete description and background distribution), (b) part of spectrum corresponding to detection of $t\,{}^3\mathrm{He}$ events.

3.4. ^{7}H isotope. In a large number of experiments devoted to studies of light neutron–rich nuclei near a drip line, the evidence of vanishing of the conventional magic numbers and appearance of the new ones is obtained [4, 76]. In particular, it follows from the experimental data on spectroscopy of helium, lithium, and beryllium isotopes that the number of neutrons $N = 6$ becomes magic rather than $N = 8$. Based on the latter, it is reasonable to expect that among superheavy hydrogen isotopes ^{7}H will turn out to be the most bound one.

An indication of the existence of the resonance ^{7}H state was first obtained in the reaction $p(^8\mathrm{He}, pp)^7\mathrm{H}$ at the ^{8}He beam's energy of 61.3 A MeV. The experiment was performed at RIKEN (Japan) in the secondary beam of radioactive ions ^{8}He [77]. The spectrum of the missing mass obtained in correlation measurements of two protons is presented in Fig. 24. The threshold of ^{7}H

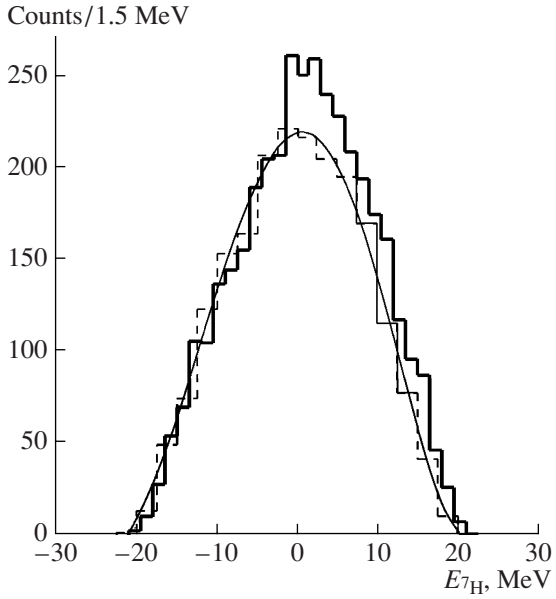

Fig. 24. Spectrum of ^{7}H from the reaction $p(^8\text{He}, pp)^7\text{H}$. Solid histogram is obtained with hydrogen target. Dashed histogram and smooth curve show background from "empty" target [77].

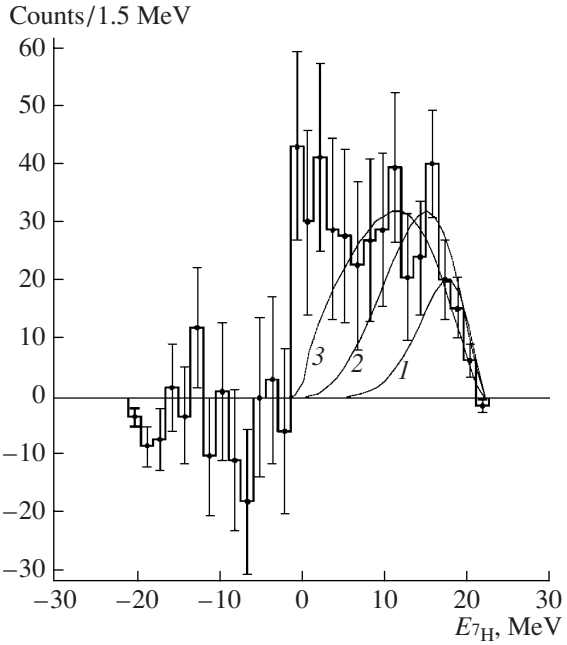

Fig. 25. Spectrum of ^{7}H after removing "empty" target background from initial spectrum. Curves *1–3* show distributions over various multiparticle phase spaces for systems with t and $4n$ [77].

breakup into system $t + 4n$ is taken to be a reference point. The solid histogram represents the spectrum measured with a proton target, whereas the dashed one displays that measured with no target at all.

It is seen in Fig. 24 that close to zero there is certain structure for positive values of missing masses in measurements with the proton target. More clearly this feature is shown in Fig. 25, where a difference in measurements with proton and "empty" targets is demonstrated. Attempts of the authors to describe the spectrum in Fig. 25 with multiparticle distributions over phase space (lines *1, 2*, and *3*) turned out to be relatively unsuccessful. Therefore, they supposed that the excess of events is due to the resonance ^{7}H state. However, with such a big background-to- signal ratio the authors could not draw any conclusions on the binding energy and the width of this state.

In [78] the search for stable and quasi–stable ^{7}H states produced in the reaction $^2\text{H}(^8\text{He}, ^7\text{H})^3\text{He}$ was carried out. However, the authors were able to obtain only an upper bound on the production cross-section of such a state of ~3 nb/sr.

In the experiment performed at LAMPF, the search for the ^{7}H isotope was performed in the spectra of the missing mass for the following channels of the reaction of stopped pion absorption:

$$^9\text{Be}(\pi^-, pp)X \quad \text{and} \quad ^{11}\text{B}(\pi^-, p^3\text{He})X.$$

In Fig. 26, the spectrum of the missing mass for the reaction $^9\text{Be}(\pi^-, pp)X$ is presented. There are no clearly seen resonance states in the spectrum which can be a result of poor statistics. Therefore, at first, an attempt was undertaken to describe this spectrum by the total distribution over the phase space with only those channels included, in which nucleon–stable nuclei and nucleons are produced.

The distribution obtained is shown in Fig. 26a. It is seen that this description is unsatisfactory (the value of $\chi^2/N_{DF} = 6.3$). A comparison with the experimental spectrum shows that it is necessary to include the channels with fewer particles in the final state.

With this aim, the channels with account for the interactions of the final state of singlet neutron pairs were included in the description of the reaction. The result obtained is displayed in Fig. 26b. The value of $\chi^2/N_{DF} = 1.15$ ($N_{DF} = 60$) indicate that the hypothesis cannot be discarded. Nevertheless, a spectrum shape in the region 10 MeV ≤ MM ≤ 30 MeV suggests the possibility of the existence of highly excited ^{7}H states. In our opinion, it is valuable to obtain information on possible location of these states. In Fig. 26c, description of the spectrum is presented, with two levels included, whose parameters of the Breit–Wigner distribution are (E_r, Γ): (16 MeV, 2 MeV) and (21 MeV, 5 MeV). It should be stressed that these results can only be viewed as indications of a possible way to search for highly excited ^{7}H states.

One of the possible reasons for the absence of high results of statistics on the observation of ^{7}H states near threshold $t + 4n$ in the reaction $^9\text{Be}(\pi^-, pp)X$ can stem from the mechanism of the latter. Our data with ^{10}B [15]

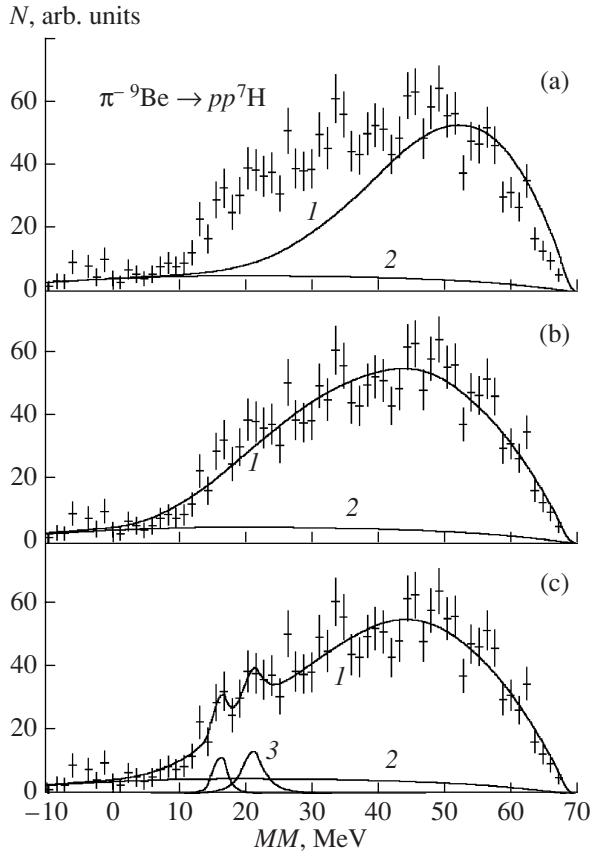

Fig. 26. Missing mass spectra for the reaction ^{9}Be(π^-, pp)X: (a) description with inclusion of (1–3) channels, (b) description with inclusion of (1–5) channels, (c) description with inclusion of (1–5) channels and two ^{7}H states. Solid lines: *1*, complete description, *2*, background coming from random coincidences, *3*, Breit–Wigner distributions.

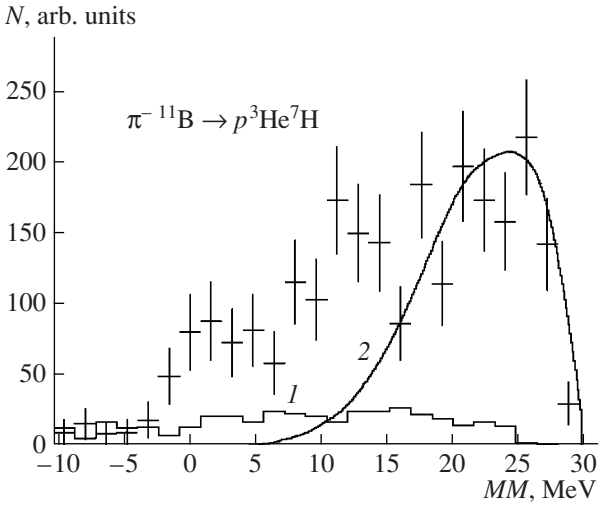

Fig. 27. Missing mass spectra for the reaction ^{11}Be(π^-, p^3He)X: *1*, normalized spectrum for the reaction ^{12}C(π^-, p^3He)X, *2*, complete description with account for only those channels in which nucleon–stable nuclei and nucleons are produced.

demonstrate selectivity of the level population in the channel of the absorption reaction with detection of two protons. There are no traces of the production of the ground ^{8}He state in the spectrum of the missing mass for the reaction ^{10}B(π^-, pp)X, whereas the peak related to the excited state with $E_x \approx 4.4$ MeV is clearly seen. The situation is opposite for other channels of the reaction of π^--meson absorption. A yield of the ground state of ^{8}He in the reactions ^{9}Be(π^-, p)X and ^{11}B(π^-, pd)X is a few times higher than that of excited states of this nucleus [31]. A more detailed discussion of the (π^-, pp) reaction mechanism is given in [15].

The spectrum of the missing mass of the reaction ^{11}B(π^-, p^3He)X is shown in Fig. 27. It is seen that the statistics are very low allowing for only qualitative conclusions to be drawn.

The events in the region of negative missing masses result from ^{12}C impurity in the target ^{11}B. The corresponding contribution of the reaction ^{12}C(π^-, p^3He)X was determined by normalizing the spectrum measured with ^{12}C in the same run to the relative portion of impurity (8%).

In the region of positive values of *MM* the most interesting aspect is the existence of a definite structure near the threshold. A sharp increase of the spectrum near $MM \approx 0$ MeV can be connected with the three-particle channel of the reaction with the almost bound ^{7}H state produced. However, the quantitative analysis of this region of the spectrum is impossible because of low statistics and poor energy resolution.

In the region of *MM* exceeding 5 MeV no structural peculiarities are found. The only point to be mentioned is that the description of this part of spectrum by only those channels, in which nucleon–stable nuclei are produced, turns out to be unsatisfactory.

So, the question of the possible existence of ^{7}H states, both near the $t + 4n$ threshold and in the region of higher excitations remains open, and new experiments to search for these states are still in demand.

CONCLUSION

Experimental results of the search for and spectroscopy of $^{4–7}$H obtained in stopped π^--meson absorption by ^{9}Be and ^{11}B nuclei considered in this review demonstrate a promising line of investigations of superheavy hydrogen isotopes. The following main results can be listed:

—ground state of ^{4}H is more bound than expected earlier;

—excited levels of isotopes ^{5}H and ^{6}H located above the threshold of breakup into free nucleons are identified for the first time;

—indication of the existence of the ^{7}H isotope near the threshold of breakup into triton and four neutrons is obtained.

At the same time, it should be noted that the experimental status of spectroscopy of superheavy hydrogen isotopes remains vague. Highly controversial is the problem of energy of the ground ^{5}H state. As was pointed out in [79], it is quite difficult to find a consistent scenario for the existing experimental data. Therefore, the contradictions present can only be resolved by new experimental information on ^{5}H.

From our results for the lowest lying states it follows that the binding energy of superheavy hydrogen isotopes is steadily decreasing with an increasing number of neutrons: $B(^4H_{g.s}) = 6.9 \pm 0.1$ MeV, $B(^5H_{g.s}) = 3.0 \pm 0.2$ MeV and $B(^6H_{g.s}) = 1.9 \pm 0.7$ MeV. Note that this inference is not influenced by uncertainty in ^{5}H energy measurements. It seems that for superheavy hydrogen isotopes the dependence of the binding energy on the number of neutrons is different from that for heavy helium and lithium isotopes, for which an even number of neutrons leads to increase in binding as being a result of neutron coupling.

The question of the nature and mechanism of production of highly excited ^{5,6}H, and perhaps ^{7}H states, is still unsettled. Analysis of the results compiled from light nuclei spectroscopy [38] shows that similar highly excited states were observed with only ^{5,6}He, and ^{5}Li isotopes in [52]. The levels with excitation energy E_x = 35.7 MeV for ^{5}He and E_x = 34 MeV for ^{5}Li are maybe isobaric analog states of ^{5}H with E_{2r} = 18.0 MeV observed in our experiment. The levels of ^{6}He with E_x = 32.0 and 35.7 MeV may similarly be isobaric analog of the ^{6}H levels with E_r = 10.7 and 15.3 MeV.

From our point of view, there are two promising lines of future investigations of superheavy hydrogen isotopes in stopped pion absorption by nuclei.

The results obtained show that the reinvestigation of the reaction ^{11}B(π^-, p^3He)X can lead to discovery of a (almost) bound ^{7}H state. Such an aim can be achieved providing statistics higher by an order of magnitude. At present, there is a chance to meet that requirement with the experiment at PSI meson factory.

The second line of investigation is related to the reaction ^{10}Be(π^-, pd)X. From the results given in Section 3.3, and the data on the spectroscopy of ^{8}He [31] and ^{11}Li [32] obtained by us, it can be inferred that the yields of three-particle channels of the reaction (π^-, pd) are sufficiently large. The main problem in this case is the production of radioactive ^{10}Be target.

ACKNOWLEDGMENTS

We are grateful to P. V. Morokhov and V. A. Pechkurov for useful discussions and valuable remarks. This work was supported by the Russian Foundation for Basic Research, project no. 07-02-00428a and the Leading Scientific School, project no. NSh–3489.2008.2.

REFERENCES

1. A. I. Baz', V. I. Goldanskii, V. Z. Goldberg, and Ya. B. Zel'dovich, *Light and Intermediate Nuclei Close to the Drip Line* (Nauka, Moscow, 1972) [in Russian].
2. I. Tanihata, J. Phys. G: Nucl. Part. Phys. **22**, 157 (1996)
3. R. Kalpakchieva, Yu. E. Penionzhkevich, and Kh. G. Bolen, Fiz. Elem. Chastits At. Yadra **30**, 1429 (1999) [Phys. Part. Nucl. **30**, 627 (1999)].
4. B. Jonson, Phys. Rep. **389**, 1 (2004).
5. A. M. Gorbatov et al., Yad. Fiz. **50**, 1551 (1989) [Sov. J. Nucl. Phys. **50**, 962 (1989)].
6. N. K. Timofeyuk, Phys. Rev. C **65**, 064306 (2002).
7. L. V. Grigorenko, N. K. Timofeyuk, and M. V. Zhukov, Eur. Phys. J. A **19**, 187 (2004).
8. S. Aoyama and N. Itagaki, Nucl. Phys. A **738**, 362 (2004).
9. R. de Diego et al., Nucl. Phys. A **786**, 71 (2007).
10. F. M. Marques et al., Phys. Rev. C **65**, 044006 (2002).
11. M. G. Gornov et al., Pis'ma Zh. Eksp. Teor. Fiz. **77**, 412 (2003) [JETP Lett. **77**, 344 (2003)].
12. Yu. B. Gurov et al., Pis'ma Zh. Eksp. Teor. Fiz. **78**, 219 (2003) [JETP Lett. **78**, 183 (2003)].
13. Yu. B. Gurov et al., Eur. Phys. J. A **24**, 231 (2005).
14. Yu. B. Gurov et al., Yad. Fiz. **68**, 520 (2005) [Phys. At. Nucl. **68**, 491 (2005)].
15. Yu. B. Gurov et al., Yad. Fiz. **69**, 1448 (2006) [Phys. At. Nucl. **69**, 1448 (2006)].
16. Yu. B. Gurov et al., Eur. Phys. J. A **32**, 261 (2007).
17. M. G. Gornov et al., Nucl. Instrum. Methods Phys. Res. A **446**, 461 (2000).
18. H. Weyer, Phys. Rep. **195**, 295 (1990).
19. G. Backenenstoss, Ann. Rev. Nucl. Sci. **20**, 467 (1970).
20. V. S. Butsev, A. S. Il'inov, and S. I. Chigrinov, Fiz. Elem. Chastits At. Yadra **11**, 900 (1980) [Sov. J. Part. Nucl. **11**, 358 (1980)].
21. R. C. Cohen et al., Phys. Lett. A. **14**, 242 (1965).
22. R. C. Mineart et al., Phys. Rev. **177**, 1455 (1969).
23. T. C. Meyer, Nucl. Phys. A **324**, 335 (1979).
24. U. Sennhauser et al., Phys. Lett. A. **103**, 409 (1981).
25. U. Sennhauser et al., Nucl. Phys. A **386**, 429 (1982).
26. M. G. Gornov et al., Pis'ma Zh. Eksp. Teor. Fiz. **45**, 205 (1987) [JETP Lett. **45**, 252 (1987)].
27. A. I. Amelin et al., Pis'ma Zh. Eksp. Teor. Fiz**. 51**, 607 (1990) [JETP Lett. **51**, 688 (1990)].
28. S. Blagus et al., Phys. Rev. C **44**, 325 (1991).
29. M. G. Gornov et al., Nucl. Phys. A **531**, 613 (1991).
30. Yu. B. Gurov et al., Pis'ma Zh. Eksp. Teor. Fiz. **84**, 3 (2006) [JETP Lett. **84**, 1 (2006)].
31. M. G. Gornov et al., Izv. RAN, Ser. Fiz. **62**, 2209 (1998).
32. M. G. Gornov et al., Phys. Rev. Lett. **81**, 4325 (1998).
33. M. G. Gornov, in *Proc. of XVth Intern. Conf. on Particles and Nuclei, Sweden, Uppsala, June 10–16, 1999*, p. 216.

34. M. G. Gornov et al., Preprint OIYaI R15-82-173 (Dubna, 1982) [in Russian].
35. A. I. Amelin et al., in *Proc. of the Intern. Workshop on Pions in Nuclei, Penyscola, Spain*, Ed. by E. Oset (World Sci., 1992), p. 516.
36. M. G. Gornov et al., Nucl. Instrum. Methods Phys. Res. **225**, 42 (1984).
37. A. I. Amelin et al., Prib. Tekh. Eksp., No. 1, 69 (1993).
38. D. R. Tilley et al., Nucl. Phys. A **708**, 3 (2002).
39. M. G. Gornov et al., Prib. Tekh. Eksp., No. 3, 55 (1994).
40. M. G. Gornov et al., Prib. Tekh. Eksp., No. 1, 57 (1988).
41. M. G. Gornov et al., Prib. Tekh. Eksp., No. 6, 42 (1983).
42. M. G. Gornov et al., Nucl. Instrum. Methods Phys. Res. A **225**, 42 (1984).
43. M. G. Gornov et al., Prib. Tekh. Eksp., No. 5, 53 (1998).
44. D. R. Tilley et al., Nucl. Phys. A **745**, 155 (2004).
45. D. R. Tilley, H. R. Weller, and G. M. Hale, Nucl. Phys. A **541**, 1 (1992).
46. J. D. Seagrave, L. Cranberg, and J. E. Simmons, Phys. Rev. **119**, 1981 (1960).
47. T. A. Tombrello, Phys. Rev. **143**, 772 (1966).
48. G. M. Hale et al., Phys. Rev. C **42**, 438 (1990).
49. A. Csoto and G. M. Hale, Phys. Rev. C **55**, 536 (1997).
50. G. M. Hale, R. E. Brown, and N. Jarmie, Phys. Rev. Lett. **59**, 763 (1987).
51. R. B. Weisenmiller et al., Nucl. Phys. A **280**, 217 (1977).
52. R. Franke et al., Nucl. Phys. A **433**, 351 (1985).
53. A. V. Belozyorov et al., Nucl. Phys. A **460**, 352 (1986).
54. D. Miljanic, S. Blagus, and M. Zadro, Phys. Rev. C **33**, 2204 (1986).
55. S. Blagus et al., Phys. Rev. C **44**, 325 (1991).
56. D. V. Aleksandrov et al., Pis'ma Zh. Eksp. Teor. Fiz. **62**, 18 (1995) [JETP Lett. **62**, 18 (1995)].
57. M. Meister et al., Nucl. Phys. A **723**, 13 (2003).
58. S. I. Sidorchuk et al., Phys. Lett. B **594**, 54 (2004).
59. A. M. Lane and R. G. Thomas, Rev. Mod. Phys. **30**, 257 (1958).
60. A. M. Badalyan et al., Yad. Fiz. **41**, 1460 (1985) [Sov. J. Nucl. Phys. **41**, 926 (1985)].
61. A. M. Gorbatov et al., Yad. Fiz. **48**, 1255 (1988) [Sov. J. Nucl. Phys. **48**, 797 (1988)].
62. K. Arai, Phys. Rev. C **68**, 034303 (2003).
63. V. D. Efros and H. Oberhummer, Phys. Rev. C **54**, 1485 (1996).
64. K. K. Seth, in *Proc. of the 4th Intern. Conf. on Nuclei Far from Stability, 1981, Helsingor* (CERN Publ., 1981–1990), p. 655.
65. D. V. Aleksandrov et al., in *Proc. of the Intern. Conf. on Exotic Nuclei and Atomic Masses, ENAM-95, Arles, France, 1995* (Editions Frontiers, Gif-sur-Yvette, France, 1995), p. 329.
66. A. A. Korsheninnikov et al., Phys. Rev. Lett. **87**, 092501 (2001).
67. M. S. Golovkov et al., Phys. Lett. B **566**, 70 (2003).
68. M. S. Golovkov et al., Phys. Rev. Lett. **93**, 262 501 (2004).
69. M. S. Golovkov et al., Phys. Rev. C **72**, 064612 (2005).
70. G. F. Filippov, A. D. Bazanov, and K. Kato, Yad. Fiz. **62**, 1763 (1999) [Phys. At. Nucl. **62**, 1642 (1999)].
71. N. B. Shul'gina et al., Phys. Rev. C **62**, 014312 (2000).
72. P. Descouvemont and A. Kharbach, Phys. Rev. C **63**, 027001 (2001).
73. D. V. Aleksandrov et al., Yad. Fiz. **39**, 513 (1984) [Sov. J. Nucl. Phys. **39**, 323 (1984)].
74. A. V. Belozerov et al., Nucl. Phys. A **460**, 352 (1986).
75. B. Parker, K. Seth, and R. Soundranayagam, Phys. Lett. B **251**, 483 (1990).
76. R. K. Gupta et al., J. Phys. G: Nucl. Part. Phys. **32**, 565 (2006).
77. A. A. Korsheninnikov et al., Phys. Rev. Lett. **90**, 082501 (2003).
78. M. S. Golovkov et al., Phys. Lett. B **588**, 163 (2004).
79. L. V. Grigorenko, Eur. Phys. J. A **20**, 419 (2004).